Aus der
Neurologischen Universitätsklinik Tübingen
Abteilung Neurologie mit Schwerpunkt Epileptologie

Elektrophysiologische Charakterisierung Epilepsie-assoziierter Defekte im *GABRA3* Gen

Inaugural-Dissertation
zur Erlangung des Doktorgrades
der Medizin

der Medizinischen Fakultät
der Eberhard Karls Universität
zu Tübingen

vorgelegt von

Scheuber, Pauline Selma

2024

Dekan: Professor Dr. B. Pichler

1. Berichterstatter: Professor Dr. H. Lerche
2. Berichterstatter: Professorin Dr. M. Knipper-Breer

Tag der Disputation: 18.12.2023

Dedicated To:

First and foremost, I would like to thank Dr. Mahmoud Koko Musa for giving me courage and guidance whenever I needed it. I owe my thanks to everyone who supported me, professionally and personally - especially Dr. Ulrike Hedrich-Klimosch, Carolin Fischer, Nikolas Layer, Simone Seiffert, Emilio Pardo Gonzales, and Moritz Hanke from the Lerche lab. I am also thankful to Prof. Dr. Lerche for giving me the opportunity to do research in his lab in the first place. To my family and friends who endured many hours of my talking about the subject matter, I am grateful for your patience and input.

Contents

1 List of Abbreviations **7**

2 Introduction **9**

2.1 $GABA_R$ - an inhibitory receptor 9

2.2 Distribution and different roles of $GABA_A$ within the brain 10

2.3 α_3-containing $GABA_A$ receptors 12

2.4 Association of $GABA_A$ receptors with genetic epilepsies and related phenotypes 15

2.4.1 A brief overview of epilepsy 15

2.4.2 Genetic epilepsies 17

2.4.3 Link between variants in genes encoding $GABA_A$ receptors and developmental and psychiatric diseases 19

2.5 Functional characterisation of $GABA_A$ receptors associated with neurological disorders 21

2.6 α_3-related neurological phenotypes 23

2.7 New variants in *GABRA3* 25

2.8 Aim of this thesis 27

3 Materials and Methods **28**

3.1 Variant evaluation 28

3.2 Molecular biology 28

3.2.1 Primer design for site-directed mutagenesis 29

3.2.2 Mutagenesis 31

3.2.3 Transformation 32

3.2.4 Sanger sequencing 33

3.2.5 Ligation of pIRES-*GABRA3*-AcGFP 33

3.2.6 Colony PCR of the pIRES construct 34

3.2.7 Maxiprep of all constructs 35

3.3 Expression in *Xenopus laevis* oocytes 37

3.3.1 DNA linearisation 37

3.3.2 RNA preparation . . . 37
3.3.3 RNA purification . . . 37
3.3.4 Preparation of *Xenopus leavis* oocytes . . . 38
3.3.5 Injection of *Xenopus leavis* oocytes . . . 39
3.3.6 Recordings using Robocyte . . . 39
3.3.7 Oocyte data analysis . . . 41
3.4 Recordings in murine neurons . . . 42
3.4.1 Cell culture . . . 42
3.4.2 Electrophysiological recordings . . . 43
3.4.3 Analysis of neuronal data . . . 46
3.4.4 Fixation of cultured cells . . . 46
3.4.5 Immunofluorescence staining and imaging . . . 46

4 Results 48
4.1 Characterisation of clinical cases and oocyte experiments . . . 48
4.1.1 Genetic evaluation of the variants . . . 48
4.1.2 Acquired clinical data . . . 52
4.1.3 Electrophysiological results in oocytes . . . 53
4.2 Neurons and imaging . . . 59
4.2.1 Spontaneous inhibitory post synaptic currents . . . 59
4.2.2 Miniature inhibitory post synaptic currents . . . 62
4.2.3 Immunostaining and imaging of transfected neurons . . . 66

5 Discussion 68
5.1 Interpretation of results . . . 68
5.1.1 Phenotypic severity of the variants related to their molecular analysis and electrophysiological recordings . . . 68
5.1.2 Loss of Function in *GABRA3* . . . 71
5.2 Gain of function as a novel disease mechanism in *GABRA3* . . . 73
5.2.1 Gain of function variants in $GABA_A$ . . . 74
5.3 The decay of sIPSCs . . . 76
5.4 Possible underlying molecular mechanisms . . . 77

5.5 Clinical implications 77
5.6 Limitations 79
5.7 Strengths 79
5.8 Future work yet to be conducted 80
5.9 Concluding remarks 81

6 Summary **82**

7 Zusammenfassung **83**

8 References **84**

9 Statement of Authorship **92**

10 Selbstständigkeitserklärung **92**

1 List of Abbreviations

aCSF	Artificial Cerebrospinal Spinal Fluid
AP-V	(2R)-amino-5-phosphonovaleric acid
ASD	Austism Spectrum Disorder
BGH	Bovine Growth Hormone
CAE	Childhood Absence Epilepsy
CMV	Cytomegalovirus
DAPI	4',6-Diamidin-2-phenylindol
DEE	Developmental and Epileptic Encephalopathy
DEPC	Diethylpyrocarbonate
DIV	Days *In Vitro*
DMEM	Dulbecco's Modified Eagle's Medium
DMSO	Dimethylsufoxide
DNA	Desoxyribonucleic Acid
dNTP	Desoxyribonucleotide Triphosphate
DRC	Dose Response Curve
DS	Dravet Syndrome
FS	Febrile Seizure
GABA	Gamma Aminobutyric Acid
GEFS+	Generalized Epilepsy With Febrile Seizures Plus
GFP	Green Fluorescent Protein
GGE	Genetic Generalised Epilepsies
HBSS	Hanks Balanced Salt Solution

JME	Juvenile Myoclonic Epilepsy
LB	Lysogeny Broth
mIPSC	Miniature Inhibitory Postsynaptic Current
NAFE	Non-Acquired Focal Epilepsy
NB	Neurobasal
NBQX	2,3-Dihydroxy-6-nitro-7-sulfamoyl-benzo[f]chinoxalin-2,3-dion
PBS	Phosphate Buffered Saline
PCR	Polymerase Chain Reaction
PDL	Poly-D-Lysin-Hydrobromide
RNA	Ribonucleic Acid
rNTP	Ribonucleic Nucleotide Triphosphate
SAP	Shrimp Alkaline Phosphatase
SEM	Standard Error of the Mean
sIPSC	Spontaneous Inhibitory Postsynaptic Current
SD	Standard Deviation
SDM	Site Directed Mutagenesis
SMEI	Severe Myoclonic Epilepsy in Infancy
Tris	Tris(hydroxymethyl)aminomethane
TTX	Tetrodotoxin
UV	Ultraviolet
WT	Wildtype

2 Introduction

2.1 GABA$_R$ - an inhibitory receptor

γ-aminobutyric acid (GABA) receptors embody one group of the many receptors mediating electrochemical processes within the brain, facilitating thought and action within living beings. In itself, it is a heterogeneous composition of different kinds of receptor subtypes that assemble to be the GABA receptor family (Sieghart & Sperk, 2002). When zooming in, one can differentiate between two large groups: GABA$_A$ and GABA$_B$ receptors. These receptors are predominantly expressed within the central nervous system (CNS). Whereas they differ on a molecular level - the first one is classified as ionotropic, or ligand-activating ion channel. The latter, on the other hand, activates a metabotropic, second-messenger intracellular pathway. However, they usually serve one common purpose: they emit inhibitory postsynaptic currents (Möhler, 2006).The ionotropic GABA$_A$ channel is opened by specific binding of the neurotransmitter GABA, making way for Chloride ions to pass into the cell, hyperpolarising it and consequentially emitting an inhibitory postsynaptic potential (Möhler, 2006).

GABA$_A$ is usually made up of five different individually translated subunits that make up the pentameric structure of the ion channel. The most prevalent combination is made up of 2 α, 2 β and 1 γ subunits (see *Figure 1*). They align clockwise as a heteropentamer consisting of γ-α-β-α-β subunits to form a functioning receptor (Sieghart & Sperk, 2002; Essrich et al., 1998). These subunits are differentiated even further into α_1 - α_6 , β_1 - β_3 , and γ_1 - γ_3. Other subunits that can be detected in place of γ are δ , ϵ , ρ_1 - ρ_3 , θ , and π (Sieghart & Sperk, 2002). Emphasizing the heterogeneity of the various

subtypes, they are encoded by 19 different genes (Fritschy & Panzanelli, 2014). Within the CNS, they're distributed in various constellations and localisations. Even if they seem so different, on a molecular level, the translated subunits share certain similarities: each one consists of four transmembrane domains. The C- and N-terminus of the protein are located on the extracellular side. The neurotransmitter binds between an α and β subunit that have aligned next to each other. Inferring from the assemblage of the respective subunits, two GABA binding sites exist in the heteropentameric structure. The channel then permits Chloride ions (Cl^-) to pass (Unwin, 1993), typically leading to hyperpolarisation of the cell.

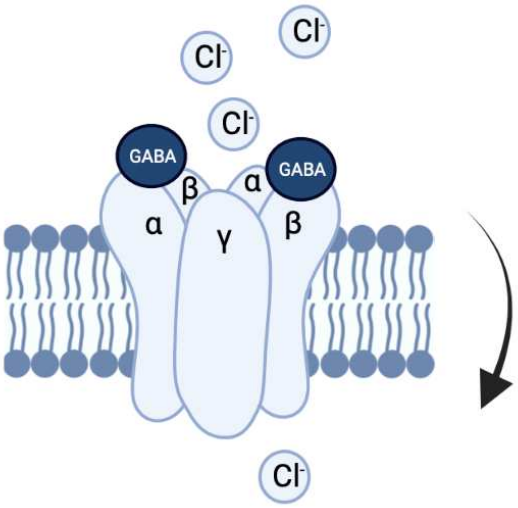

Figure 1. Schematic structure of a pentameric ionotropic $GABA_A$ receptor formed of 2 α, 2 β and 1 γ subunits.

2.2 Distribution and different roles of $GABA_A$ within the brain

Ben-Ari introduced the theory that during early development, activation of GABA receptors might lead to depolarisation, rather than the classical hyperpolarisation (Ben-Ari,

2002). It is also implied that the general activation of GABA receptors is vital for synapse development. As both glutamatergic and GABAergic neurons are largely present during development (Behuet et al., 2019), it is suggested that neuron migration is affected by this intricate system. Co-localisation of GABA with synaptophysin - a vesicular protein located typically in the presynapse (Wiedenmann et al., 1986) - was also observed. This underlines the suggestion of the influence GABA has on the formation of synapses. Consequentially, neural networks within the developing brain are furthermore influenced by GABA activity (Hutcheon et al., 2004). Still, this interplay of molecules and their receptors has not yet been studied well enough to derive a generalisation.

Moving on from prenatal development and the hypothesis that GABA can fulfil an excitatory purpose within the CNS, $GABA_A$ receptors are still understood to serve as the main inhibitory receptor in the adult brain. One can differentiate between tonic and phasic inhibition. Phasic inhibition describes whether the channel has been opened by binding of a transmitter - GABA - which has been previously released by presynaptic vesicles. Contrasting that in the case of tonic inhibition, there is also the possibility of extrasynaptic activation (Farrant & Nusser, 2005). It is less temporally and spatially determined, as the receptors are located outside of the synaptic cleft. Both means of inhibition are possible in the case of $GABA_A$. Conductance for Cl^- ions seems to differ as well for the two states described above. Regarding phasic inhibition, there is a fixed time frame in which the receptor opens and facilitates the membrane permeability of Cl^- ions, hyperpolarising quickly with a brief increase in concentration (Farrant & Nusser, 2005).

As we've established, the GABA receptor family is more complex than it appears at first

glance. The variety of GABA$_A$ subunits suggests a diverse range of functions, possibly depending on different brain regions. It is known that the receptor groups appear ubiquitously within the CNS. Yet, the various subtypes that align into pentamers differ greatly depending on their respective localisation; Pirker and colleagues (Pirker et al., 2000) have studied the localisation and constellation of the various subunits and concluded that β_2 and γ_2 appear to be a common combination. Furthermore, the most commonly found subtype within the α group is α_1, closely followed by α_2 and α_3.

2.3 α_3-containing GABA$_A$ receptors

This thesis will focus on α_3. α_3 is encoded on the *GABRA3* gene which is located on chromosome Xq28 (National Center for Biotechnology Information, 2021). The translated protein consists of 492 amino acids, with the signal peptide being located at amino acid 29 – 276. It is preceded by a long extracellular N-terminus at amino acids 1 - 28. The four helical transmembrane domains are expressed by the amino acids in 277 – 298, 304 – 325, 338 – 359, and 458 – 479th position. In between the topological transmembrane domains 3 and 4, there is one large intracellular domain spanning amino acids 360 – 457 (UniProt Consortium, 2021). *Figure 2* depicts a schematic overview of the respective amino acids that make up the protein as it appears in the cell membrane. α_3 remains expressed before and after birth in mice (Laurie et al., 1992), which implies a certain significance of the receptor subtype before and after birth. Still, one needs to consider that conclusions about the purpose during development cannot be drawn liberally. When studying functional brain regions using selective antibodies, one is able

to observe α_3 within the cingulate, frontal, occipital cortex, brain stem as well as the midbrain. (Fritschy & Mohler, 1995). Moreover, the reticular nucleus of the thalamus, Amygdala, locus coeruleus, as well as the reticular formation especially express that subunit. Within the islands of Calleja, the subunit aligns with γ_2 (Fritschy & Mohler, 1995). These localisations all project into the dopaminergic system, which may have interesting implications for the function of α_3. Especially considering it is the only α subunit to be expressed within the substantia nigra (Rodríguez-Pallares et al., 2001), it may serve a curious function within the dopaminergic system of the brain. Contrasting these aforementioned areas, where α_3 is predominant, it is not one of the cardinal proteins within the brain region that contains a vast amount of $GABA_R$, the hippocampus (Hutcheon et al., 2004).

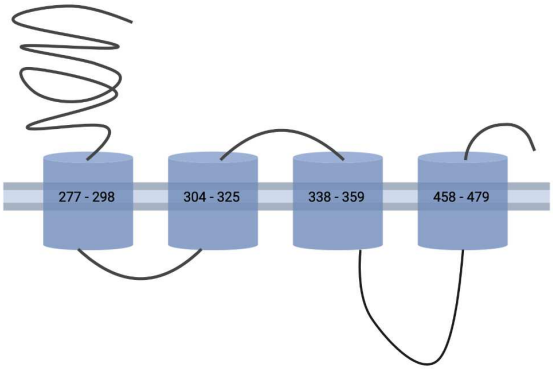

Figure 2. The α_3 subunit as it is integrated into the cell membrane. The amino acids making up the transmembrane domains are labeled.

Not only does α_3 seem to appear quite often within the brain (in 10-15 $\%$ of $GABA_A$ receptors as a broad estimate (Sieghart & Sperk, 2002)). The subunit also serves a pharmacological purpose. It has a benzodiazepine binding site - when aligned with a β subunit (Christian et al., 2013). Like this, it is able to be modulated on a biochemical level, being activated in an allosteric way and therefore letting more anions (mainly Cl^-) pass through the channel. α_3 especially portrays a high affinity for classical benzodiazepine agonists and flumazenil, an antagonist. Zolpidem, on the other hand, appears to show less of a strong binding capacity for the subunit (Möhler, 2006). Being expressed in such high numbers within the brain and having the advantage of having very specific binding sites, it could be used in an advantageous manner when altering receptor properties. For example, certain pathologies affecting the function of a specific subtype could be targeted pharmacologically. Perhaps adverse effects of medications could be minimised as much as possible.

In the case of α_3 in combination with γ_2, it seems as though the formed pentamer is mostly described as a postsynaptic receptor, indicating a role of a phasic inhibitory channel; this phasic activation is associated with generating oscillating activities within neural networks (Farrant & Nusser, 2005). Because this mechanism is relevant for neurological pathologies, such as epileptic and developmental phenotypes (Niturad et al., 2017), it is necessary to investigate the electrophysiological properties (and accompanying that the temporal activation of the channel) of α_3. Consequently, coexpression of the additional subunits is imperative to simulate its function in heterologous expression systems *in vitro* (e.g. *Xenopus laevis* oocytes or HEK cells). Studies have found that two α_3 subunits most commonly align with two β_2 and one γ_2 subunits to form a functioning

ion channel (Fritschy et al., 1992). Alternatively, neuronal cultures or model organisms such as knock-out mice might offer a more advanced approximation to the physiological and pathological conditions. In these cases, additional subunits are already endogenously expressed.

2.4 Association of $GABA_A$ receptors with genetic epilepsies and related phenotypes

2.4.1 A brief overview of epilepsy

Epilepsy describes a neurological condition which affects about 50 million people in the world to date (World Health Organization, 2021). To be diagnosed formally, at least two seizures in an unprovoked manner are to occur with a minimal gap of a day apart from each other (Fisher et al., 2014). Another criterion is that the likelihood of another seizure occurring within 10 years must lie above 60 $\%$. This probability can be approximated by brain lesions in an MRI image, or epilepsy-typical potentials in an electroencephalography (EEG) recording. Alternatively, a corresponding syndrome is required to have been diagnosed in the past. Only then does the condition qualify as epilepsy. A seizure, in turn, is caused by abnormal or synchronous activity within the brain, leading to transient symptoms with a clear onset and ending (Fisher et al., 2014). It can be detected by changes in behavior or by a distinct presentation when conducting a recording of EEGs. Depending on the part of the brain affected, various types of senses can present themselves as being altered during the seizure. These include motor function, smell, or vision, among others (Fisher et al., 2014). A corresponding pattern

can also be detected within the EEG in the affected brain areas, underlining the physical localisation or origin of the seizure.

A variety of clinical presentations within patients is possible. Hence, depending on the type of onset of the seizure, the symptoms are further classified into focal (restricted to a circumscribed area, usually originating in the hippocampus), generalised, or epilepsies with an unknown origin in the broadest sense (Fisher et al., 2017). Still, even generalised epilepsies usually originate from one part of the brain, moving on to dominate the EEG recordings. The subtypes are further broken down into motor vs. non-motor seizures with or without loss of awareness. As complex as motor or non-motor reactions can be, they are differentiated once more depending on the precise clinical symptoms (Scheffer et al., 2017).

The pathophysiology of this complex condition remains to be clarified as of now. Yet, the oscillation or synchronous activity of electric currents is due to neural networks being activated and spreading - at least in the case of generalised epilepsy (Bromfield et al., 2006). It is known that the interconnection of neurons is due to electrochemical changes between the cells, altering the firing of associated neurons. Therefore, it can be inferred that an imbalance in regulating factors might be at the root of epilepsy. This has been associated in previous studies with voltage and ligand-gated channels, mediating the inhibitory and excitatory potentials generated between the cells transmitting information. One of these is the group of GABA receptors (Tasker & Dudek, 1991), as it causes post-synaptic inhibitory potential. This is only one example, though: other receptors have also been associated with epilepsy. These include NMDA, several potassium, or sodium channels (Weber & Lerche, 2008). Staying at the level of impaired receptor function,

it is vital to explore the origin of their malfunction. Furthermore, an association to the clinical presentation of epilepsy is desirable when trying to find the root of the symptoms in these ion and voltage gated channels.

2.4.2 Genetic epilepsies

For almost half of epilepsies, a genetic cause can be identified. In some cases, the root can be traced back to specific receptors, as mentioned in the previous section. In that case one can explain the epileptic symptoms by the expression of dysfunctioning voltage gated or ligand activated channels which impair the ion regulation within the brain (Lerche et al., 2013). This rattles up the carefully maintained equilibrium of the well-working nervous system, disturbing its neural networks and leading to epileptic seizures or syndromes. The fact that the associated channel may not work properly can be caused by genetic variants. The exact variants within channels have been discovered by the use of sequencing studies for individuals. Association studies have in turn contributed to the identification of the impaired loci on chromosomes. The advantage is that in this scenario, a vast amount of patients can be studied. In turn, overlaps in genetic variations can reliably be associated with epileptic syndromes (Epi4K Consortium & Epilepsy Phenome/Genome Project, 2013; Weber & Lerche, 2008). Furthermore, entire families can be inspected on a genetic level. That is useful when trying to pinpoint inherited epilepsy. Monogenic (single risk gene) as well as polygenic causes have been discovered.

One of the first variants to be described and associated with generalised epilepsy and febrile seizures are two rare variants within the γ_2 subunit (Wallace et al., 2001; Baulac

et al., 2001). So far, genetic variations of the *GABRA1* (Cossette et al., 2002), *GABRA2* (Butler et al., 2018), *GABRA3* (Niturad et al., 2017), *GABRA5* (Butler et al., 2018), *GABRB2* (Srivastava et al., 2014), *GABRB3* (Møller et al., 2017), *GABRG2* (Baulac et al., 2001), and *GABRD* (Ahring et al., 2021) genes have been traced back to epileptic phenotypes or associated diseases (Macdonald et al., 2010). These phenotypes include a broad spectrum of childhood absence epilepsy (CAE), juvenile myoclonic epilepsy (JME), febrile seizures (FS), generalised epilepsy with febrile seizures plus (GEFS+), Dravet syndrome (DS)/severe myoclonic epilepsy in infancy (SMEI), and generalised genetic epilepsy (GGE) not sub-classified as CAE, JME, or another syndrome. As diverse as the described variants are, the syndromes associated with respective subunits also vary widely. Collectively, variants affecting genes encoding $GABA_A$ receptors are enriched in genetic generalised epilepsies and non-acquired focal epilepsies (May et al., 2018; Epi25, 2019). Some of the phenotypic associations with epilepsy are visualised in *Table 1*.

Encoding Gene	Epilepsy Phenotype
GABRA1	GGE (JME, CAE)
GABRA2	DEE
GABRA3	DEE
GABRA5	DEE, GGE
GABRB1	DEE
GABRB2	DEE, GGE
GABRB3	GGE (CAE), GEFS+, DEE
GABRG2	DEE, GGE (CAE), FS, GEFS+, NAFE
GABRD	GEFS+, GGE (JME), DEE

Table 1. List of identified clinical conditions corresponding to genes encoding $GABA_A$ subunits (Kang & Macdonald, 2009; Khair & Salvucci, 2021; Maljevic, Møller, et al., 2019; Møller et al., 2017; Ahring et al., 2021; Niturad et al., 2017; Maljevic, Keren, et al., 2019; Butler et al., 2018; May et al., 2018; El Achkar et al., 2021; Epi4K Consortium & Epilepsy Phenome/Genome Project, 2013). CAE: Childhood Absence Epilepsy, DEE: Developmental and Epileptic Encephalopathy, FS: Febrile Seizure, GGE: Genetic Generalised Epilepsies, GEFS+: Generalized Epilepsy With Febrile Seizures Plus, JME: Juvenile Myoclonic Epilepsy, NAFE: Non-Acquired Focal Epilepsy.

2.4.3 Link between variants in genes encoding $GABA_A$ receptors and developmental and psychiatric diseases

By now, different clinical phenotypes other than genetic epilepsies have been associated with abnormal function of $GABA_R$ within the brain (Kang & Barnes, 2013). The clinical phenotype of schizophrenia has been associated with mutations within the receptor

(Jacob et al., 2008; Lewis & Gonzalez-Burgos, 2006), just to name one example. Studies of molecular pathways have implied that GABA reuptake and synthesis is decreased in schizophrenic patients, leading to a compensatory upregulation of postsynatic receptors (Lewis & Gonzalez-Burgos, 2006). Other psychiatric conditions include autism spectrum disorder (Buxbaum et al., 2002). Gene association studies were able to explain the occurrence of autism in patients by relating it to polymorphisms in *GABRA4* (Ma et al., 2005). Moreover, Angelman syndrome as a chromosomal aberration leading to autism-like behaviour and seizures in patients could also be related to alterations in GABAergic pathways (DeLorey et al., 1998). As these phenotypes are often times affiliated with developmental disorders, recent studies have shown that patients exhibiting intellectual disability in general, learning disabilities, and coordination difficulties express specific variants within the *GABRA3*, *GABRA2*, *GABRA5*, or *GABRD* gene (Niturad et al., 2017; Butler et al., 2018; Ahring et al., 2021). In most cases, these clinical presentations coincide with ASD and/or epilepsy. Interestingly, the phenotypes of variants even within one receptor subtype were found to be quite heterogeneous; for instance, *GABRD*-related clinical symptoms span from mild intellectual difficulties to patients not being able to walk at the age of three (Ahring et al., 2021). The cases where *GABRD* alterations showed a gain in function when studied *in vitro* expressed rather severe phenotypes. Difficulties in learning were present and prominent in most cases across variants. Depicted below is an overview of the various clinical conditions associated with variants of $GABA_A$ subunits as described within literature.

Encoding Gene	Associated Phenotype
GABRA1	schizophrenia
GABRA2	ASD, NDD, addiction
GABRA3	NDD with or without epilepsy
GABRA4	ASD
GABRA5	NDD
GABRA6	schizophrenia, addiction
GABRB2	ASD, schizophrenia
GABRB3	ASD, addiction
GABRG1	addiction
GABRG2	schizophrenia
GABRG3	Alzheimer's disease, ASD
GABRR2	ASD, addiction
GABRD	NDD with epilepsy, ASD

Table 2. List of identified clinical conditions corresponding to genes encoding $GABA_A$ subunits (Yuan et al., 2015; Niturad et al., 2017; Khair & Salvucci, 2021; Ahring et al., 2021; Ma et al., 2005). ASD: Autism Spectrum Disorder, NDD: Neurodevelopmental Disorder.

2.5 Functional characterisation of $GABA_A$ receptors associated with neurological disorders

As established, variants in several subunits of *GABRA* have been associated to neurological as well as psychiatric disorders. This relation can be accentuated by support of

electrophysiological data. Inferences from altered electrophysiological properties (such as differences in GABA sensitivity) can be drawn to the corresponding clinical phenotype. For that, *in vitro* studies are convenient. Several cellular expression systems are commonly used: for $GABA_R$, *Xenopus laevis* oocytes appear quite often within literature (Niturad et al., 2017; Harkin et al., 2002). In that case, the mRNA of the subunits needed are injected into the oocyte. After an incubation time of three to four days, pentameric receptors have formed. Their current responses can be recorded. In order to reach conclusions about the electrophysiological properties of the variants, their current responses are compared to the wildtype condition. The previously described works yield significantly reduced GABA currents in their variants when normalised to the WT (Niturad et al., 2017).

Another possibility is the cultivation of HEK cells, transfecting them with the DNA of the subunits (Syed et al., 2020; Cossette et al., 2002). In this case, one needs to select an appropriate transfection reagens. It might be useful to tag the isolated desired subunit with fluorescence to ascertain the cells expressing the transfected DNA.

Moving on from there, one more opportunity is to cultivate neurons *in vitro* and to transfect them with the desired subunit DNA, as it has been previously described by Eugène and his colleagues (Eugène et al., 2007).

To reach conclusions from these previously described cell expression systems, there are two possibilities: since the $GABA_A$ receptor is a ligand-gated channel, one can apply the transmitter to the cells to obtain evoked currents, as is easily performed in oocytes. By applying different concentrations of GABA, one can infer the ability to respond and sensitivity of the receptor. In neurons, electric currents that are emitted spontaneously

within the neural network can be recorded (Eugène et al., 2007).

2.6 α_3-related neurological phenotypes

In WAG/Rij rats with an absence model presenting an epileptic phenotype, a distinct change in the α_3 subunit could be observed (Liu et al., 2007). That might indicate that dysfunction of the receptor could be associated to the pathogenesis of epilepsy. In that particular study, however, the receptor could still be discovered at its designated transmembrane sites when applying methods of immunostaining within the cortex, but not in the nucleus reticularis of the thalamus. Following that, one can infer that a functional impairment is relevant in this case of disease mechanism.

Furthermore, more recently, variants within the *GABRA3* gene have been identified in patients (Niturad et al., 2017). Differing clinical symptoms were present, depending on the variant itself. However, usually some kind of developmental disorder of varying severity with or without epileptic seizures was observable in these patients. By means of *in vitro* studies, the observed phenotypes could be plausibly explained by the variants. Since the encoding gene of *GABRA3* is located on the X chromosome, the fact that male patients were showing more severe symptoms stands to reason, as they only have one X chromosome. The mutations did not have complete penetrance in their inheritance pattern. That is why a complex causality corresponding to the presented conditions is suggested. These in turn were heterogeneous with symptoms such as different epileptic seizure types, intellectual disability, and developmental delay. In some cases they were combined with dysmorphic features or nystagmus. To ensure that this was not associated with a dysfunction of the α_3 receptor subunit by chance, its functionality was studied

in vitro. *Xenopus laevis* oocytes were injected with the RNA of the α_3, β_2, and γ_2 subunits. Accordingly, the receptors were expressed in that model. After that, their electrophysiological currents were recorded using two electrode voltage clamp. Compared to receptors expressing the wildtype of α_3, current response to stimulation with GABA was reduced in case of the cells containing variant receptors. Based on this observation, a loss of receptor function could be concluded. In three out of five mutations, however, GABA sensitivity was increased (see *Table 3*). Overall, the study led to *GABRA3* being established as a new gene associated with epilepsy and neurodevelopmental disorder.

Variant	Type of epileptic seizures	Disease presentation
p.(Gly47Arg)	not defined	speech onset at age 6; autism spectrum disorder
p.(Thr166Met)	absence seizures or no seizures	micrognathia, learning disability, moderate intellectual disability, hyperactivity, speech defect (delayed onset), impaired visual-motor integration, nystagmus
p.(Gln242Leu)	tonic-clonic and spasms	cleft palate, nystagmus, microretrognathia, developmental delay, learning/intellectual disability, delayed walking and speech
p.(Thr336Met)	generalised tonic-clonic	N/A
p.(Tyr474Cys)	complex, tonic-clonic	speech defect, anxiety, generalised fear, delayed speech, intellectual disability, autism-like symptoms

Table 3. Overview of known *GABRA3* mutations and their epileptic phenotypes, plus additional behavioral and morphological conspicuities (Niturad et al., 2017).

It is most curious that such different phenotypes can all be associated with loss of function variants in the *GABRA3* gene (see *Table 3*). As it is widely spread across the CNS, its multifaceted functions might emphasise clinical complexity. So far, gain of function mechanisms have not been established clearly yet. Even though a few variants showed some increased sensitivity, the emphasis was always set on the decreased overall current response within the *in vitro* experiments. Electrophysiologically, these past studies have mainly reported decreased currents but mixed results concerning the dose response curve of variants compared to their wildtype (Niturad et al., 2017). The authors concluded that these results correlated partially with the severity in disease. To get a clearer sense of the gene and its effect on the phenotype, it might be interesting to study further variants.

2.7 New variants in *GABRA3*

We identified four new missense mutations within the *GABRA3* gene through a network of collaborators. Their localisation within the translated ionotropic receptor is schematically exemplified in *Figures 3A and 3B*. The p.(Asp115Glu) variant has been discovered in a family with neurodevelopmental disorder. Another one, p.(Tyr243Cys) is expressed by a female patient with dysmorphisms, well controlled epileptic seizures, mild brain abnormalities, and moderate intellectual disability. p.(Val309Leu) has been described in a female patient as a *de novo* mutation. Finally, p.(SerS393Ile) could be discovered in a male patient where it was maternally inherited. These variants are exemplified in *Figure 3A* and set into perspective among the previously characterised variants by Niturad and colleagues from their 2017 study in *Figure 3B*.

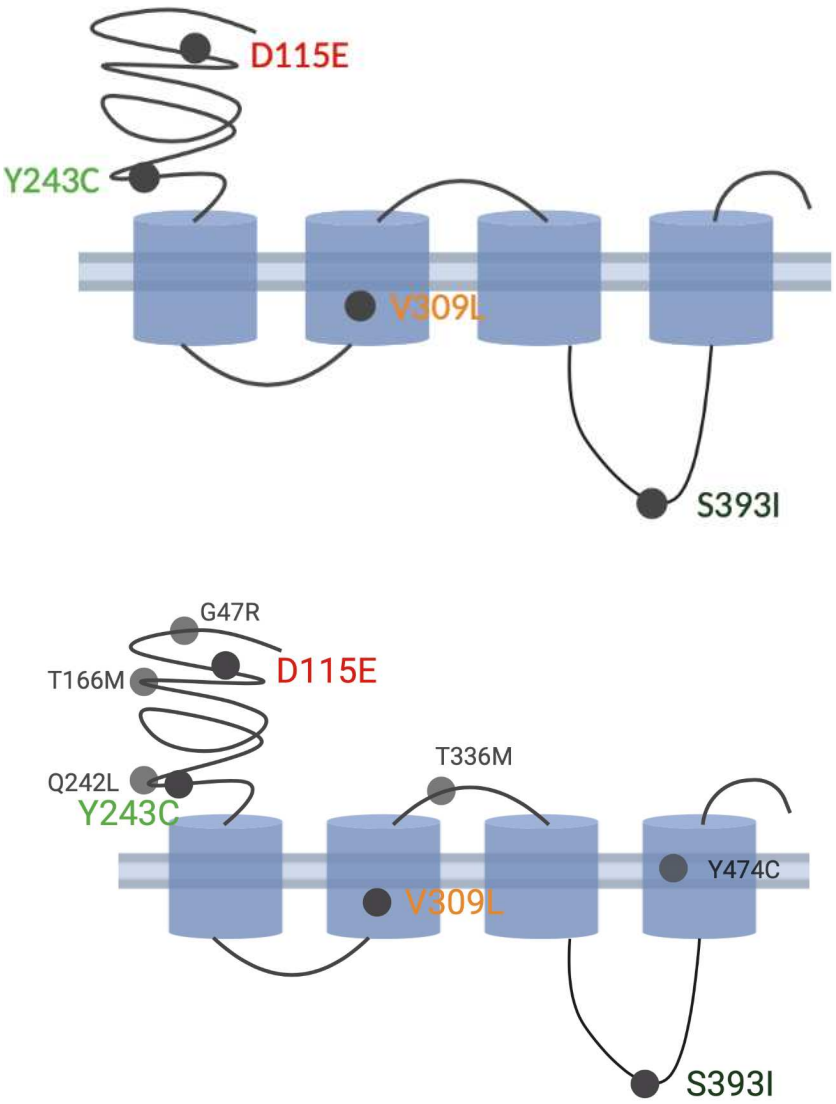

Figures 3A and 3B. Localisations of the GABA$_A$ α_3 subunit variants with its four transmembrane domains, and the intracellular loop. *Figure 3A* depicts the variants to be characterised in this thesis, *Figure 3B* provides an overview of all known variants, including the ones that have already been established to be pathogenic.

2.8 Aim of this thesis

Now that four new variants have been identified, it was first and foremost interesting to investigate whether they express a similar loss of function compared to previous variants (Niturad et al., 2017) when studied *in vitro*. This is why they were expressed in oocytes and characterised on an electrophysiological level. As the new variants show heterogeneous and new clinical phenotypes, they enlarge the phenotypical spectrum of *GABRA3*-associated disease. Another aim was to correlate the chemical phenotypes to the electrophysical dysfunction.

Still, isolated cells do not properly mirror the complexity of the brain and its neural connections. This is why we decided to express the α_3 variants in murine neurons within a neural network as a means to approximate a more realistic environment. Their spontaneous inhibitory postsynaptic currents (sIPSCs) as well as miniature inhibitory postsynaptic currents (mIPSCs) should be recorded. Like this, electrophysiological properties and response within the network could be inferred.

Accordingly, the specific objectives were as follows:

1. To describe the phenotypic spectrum of novel *GABRA3* variants.
2. To characterise the functional effects on the *GABRA3* variants using *Xenopus laevis* oocytes.
3. To record mIPSCs and sIPSCs in murine neuronal cultures transfected with *GABRA3* variant DNA, as well as staining the patched cells.

3 Materials and Methods

3.1 Variant evaluation

Variant Effect Predictor (McLaren et al., 2016) was used to annotate population allele frequencies from gnomAD Release 2.1 (Karczewski et al., 2020), TOPMed Release Freeze 8 (Taliun et al., 2021), and DiscovEHR Release Freeze 50 (Dewey et al., 2016). Additionally, conservation (GERP++ RS (Davydov et al., 2010), Para-Z-Score (Lal et al., 2020)), deleteriousness (CADD (Rentzsch et al., 2019), PPh2 (Adzhubei et al., 2010), REVEL (Ioannidis et al., 2016)), and constraint scores (MTR (Traynelis et al., 2017), MPC (Samocha et al., 2017)) were obtained. Following functional characterisation in oocytes (see below), the variants were classified using the American College of Medical Genetics and Genomics (ACMG) Classification (Richards et al., 2015).

3.2 Molecular biology

As the first step to investigate the electrophysiological characteristics of the variants, they needed to be modified using site-directed mutagenesis (SDM). Appropriate DNA vectors corresponding to the chosen expression systems were selected (oocytes, neurons). For the oocytes, pcDNA3.1 with a T7 promotor was used, as a *hGABRA3* wildtype (*Figure 4*) was already available within the laboratory from previous studies (Niturad et al., 2017). Mutations were generated by SDM. Concerning the transfection in murine neurons, a fluorescent protein was necessary: neurons expressing the α_3 subunit had to be distinguished from non-transfected neurons. A pIRES-AcGFP backbone with a CMV promotor was chosen and the WT construct was cloned. Subsequently, the mutations

were introduced by SDM.

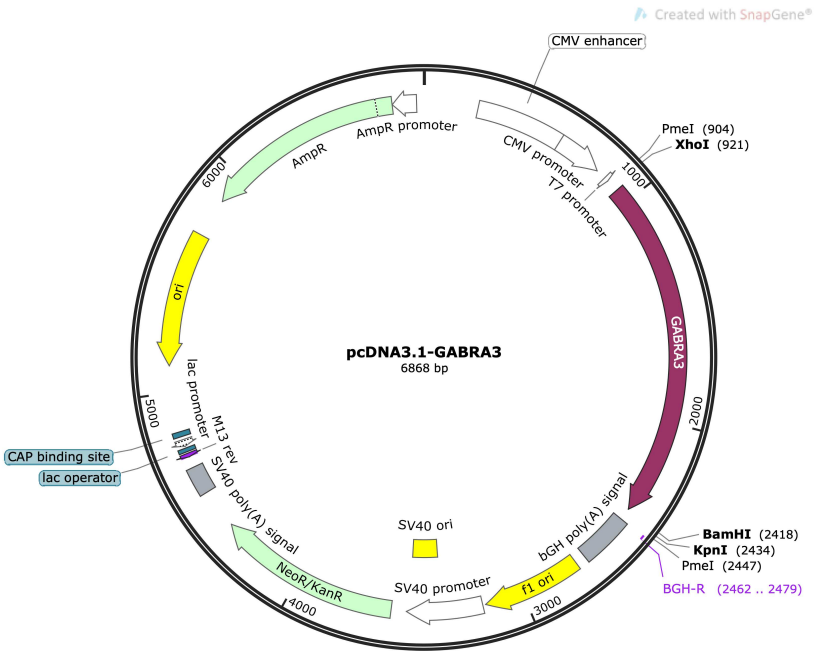

Figure 4. pcDNA3.1 construct with *GABRA3*, as used in the experiments. Relevant restriction enzyme sites are labeled.

3.2.1 Primer design for site-directed mutagenesis

To be able to characterise the four missense mutations within the *hGABRA3* gene, site-directed mutagenesis had to be performed. They were located at c.345T>A (p.D115E), c.728A>G (p.Y243C), c.935G>C (p.V309L), and c.1178G>T (p.S393I) within the gene (the transcript NM_000808.4, (National Center for Biotechnology Information, 2021)). The same primers were used for both vector constructs (pcDNA3.1 and pIRES-AcGFP). They were ordered from Integrated DNA Technologies, Inc. (IDT, Belgium).

Name	Sequence
p.D115E-F	5'- GAC ATG GAG TAC ACT ATT GAA GTA TTT TTT CGG CAG ACA TG -3'
p.D115E-R	5'- CAT GTC TGC CGA AAA AAT ACT TCA ATA GTG TAC TCC ATG TC -3'
p.Y243C-F	5'- CTT GAA CCA GTG TGA CCT TTT GG -3'
p.Y243C-R	5'- CCA AAA GGT CAC ACT GGT TCA AG -3'
p.V309L-F	5'- TGC CCG TAC ACT CTT TGG TGT C -3'
p.V309L-R	5'- GAC ACC AAA GAG TGT ACG GGC A -3'
p.S393I-F	5'- GCA AAG AAA ACC ATC ACT ACC TTC AAG -3'
p.S393I-R	5'- GTT GAA GGT AGT GAT GGT TTT CTT TGC -3'

Table 4. Designed primers used for site-directed mutagenesis and sequencing. F: forward primer, R: reverse primer.

Below, additional general purpose primers used are listed. These were used for sequencing and/or cloning purposes.

Name	Sequence
T7	5'- TAA TAC GAC TCA CTA TAG GG -3'
BGH-R	5'- TAG AAG GCA CAG TCG AGG -3'
CMV-F	5'- CGC AAA TGG GCG GTA GGC GTG -3'
IRES-R3	5'-CCT CAC ATT GCC AAA AGA CG

Table 5. List of backbone-binding primers used for sequencing and/or cloning.

3.2.2 Mutagenesis

The mutagenesis on α_3 in pcDNA3.1 was achieved by performing a polymerase chain reaction (PCR) with PfuTurbo polymerase (Agilent Technologies). The reaction mix contained 5 ng/µl of WT DNA, 0.5 nM/µl of each corresponding forward and reverse primer, 0.077 U/µl PfuTurbo polymerase (1.5 U), 3 % DMSO, 0.5 µM/µl dNTPs, topped off with 2µl of 10x reaction buffer and H_2O to receive a final volume of 20 µl. The PCR was performed as follows:

Step 1: 95°C 10 min - denaturation

———————————————————————-

Step 2: 95°C 30s

Step 3: 62°C (for all except D115E - 67°C) 30s for 18-25 cycles - annealing of primers

Step 4: 72°C 8 min - extension of DNA

———————————————————————-

Step 5: 72°C 15 min - final extension

Step 6: 4°C

An aliquot with 2 µl of the product was checked on a gel made of 1 % agarose in Tris/Borate/EDTA and 20.000 x Red Safe Dye using gel electrophoresis. For imaging, a gel documentation system with fluorescent light was used. After that, 1 µl of DpnI enzyme was added to the original PCR product. The reaction mix was incubated at 37°C for one hour to digest methylated plasmids (template plasmid), while retaining the unmethylated PCR products. Again, the obtained product was checked using gel electrophoresis.

3.2.3 Transformation

The PCR products (containing the variants) were transformed into competent bacteria. In the case of the pcDNA3.1 for D115E, Y243C, and S393I α-select bacteria were used, for the pcDNA3.1 V309L mutation TOP10 bacteria were chosen for the transformation. The choice was based on availability of bacteria at the time of experiments. The *E. coli* were taken from -80°C onto ice and left to chill for 15 minutes. Then, 10 ng of DNA was added and incubated for 30 minutes. After that, the bacteria were heat-shocked at 42°C for exactly 30 s and taken back onto ice for 2-5 minutes. After emulsifying with 250 µl of SOC medium (Thermo Fisher), the transformed bacteria were shaken at 300 rpm at 37°C for another hour before being plated onto agar plates. The construct expressed an Ampicillin resistance. Following that, the bacteria were plated on Ampicillin agar plates and incubated at 37°C overnight (100 µg/ml). The next day, colonies were picked and added to 5 ml LB medium with their corresponding antibiotic (Ampicillin, 100 µg/ml). They were put into a shaking incubator (at 37°C and 170 rpm) for another day to let the bacteria grow further.

Some of the bacteria were used to prepare glycerol stocks and stored at -80°C. The rest was processed to extract the DNA using the Extractme Plasmid Mini Kit (BLIRT S.A.) according to the manufacturer's instructions: First, the bacteria were spinned at 4,000 g for 5 minutes. The liquid was discarded and the pellet suspended in 250 µl of Suspension buffer. Then, 250 µl Lysis Buffer was added to breakup the cell membranes and left for 2 minutes. To avoid supercoiled DNA, 350 µl of Neutralisation Buffer was added, inverting the tube gently several times. At 11,000 g the mix was centrifuged for 10 minutes. Pipetting the supernatant onto a filter on a tube, the product was spinned

at 11,000 g for another minute. For the purpose of purification, the filtered product was supplied with 750 µl Wash Buffer, centrifuging once again at 11,000 g for 60 seconds. Discarding the liquid, the spinning process was repeated for 2 minutes without adding any other solutions. Using a new collection tube, 25 µl of Elution Buffer was added to the filter now containing purified DNA and incubated for 60 seconds at room temperature. In a final centrifuging process of 60 seconds at 11,000 g, the extracted DNA product was collected in the tube. Concentrations of the isolated products were obtained using Nanodrop (Thermo Fisher).

3.2.4 Sanger sequencing

The extracted DNA was sequenced to check whether the mutagenesis had worked and could be reliably used in further experiments. Sanger sequencing was provided by LGC Genomics. The primers used are detailed in Tables 4 and 5. To check the received sequences, CLC Sequence Viewer 8 (QIAGEN Bioinformatics) and SnapGene Viewer 5.2.4 (SnapGene) were utilised. The sequences were aligned with NCBI's nucleotide sequences of the *GABRA3* WT, version NM_000808 (National Center for Biotechnology Information, 2021).

3.2.5 Ligation of pIRES-*GABRA3*-AcGFP

For the fluorescent construct, the WT construct was amplified from pcDNA3.1 backbone and inserted into a pIRES-AcGFP vector. This cloning process was done by first amplifying the α_3 subunit encoded in the pcDNA3.1. For this, a PCR using HotStart MyTaq Polymerase (Bioline) was performed. Using T7 and BGH-R as forward and reverse primers, the reaction took place according to the manufacturer's instructions. For

further use as part of the ligation, the product was digested overnight using XhoI and BamHI restriction enzyme (1 µl each) with 5 µl of Cutsmart buffer (NEB). The same procedure was applied to the pIRES backbone. The next day, the vector construct was additionally dephosphorylated with 1 µl of SAP for 1 hour. Both were purified using Phenol/Chloroform extraction (see RNA Purification below).

The ligation was prepared with 1 U/µl DNA of T4 polymerase (NEB), with 10 times the volume of T4 buffer (NEB). Again, the assay was filled up with water to a total amount of 20 µl with. The insert to backbone relation was chosen at 2.5:1 and left at 4°C overnight. Control trials were conducted as well, leaving out one component of the reaction at a time and checked on an agarose gel the next day.

The ligated constructs were transformed into chemically competent NEB's DH5-α *E. coli*. A standard chemical transformation protocol was followed identical to the one elaborated above. The pIRES construct expressed a Kanamycin resistance gene. Accordingly, the bacteria were plated on an agar plate containing Kanamycin (50 µg/ml).

3.2.6 Colony PCR of the pIRES construct

To ensure an efficient ligation of α_3 WT and pIRES, colony PCRs were done using MyTaq HS (Bioline), IRES-R, and CMV-F primers. Picked colonies that had been eluted in 6 µl SOC Outgrowth Medium were used. The PCR products were checked on an agarose gel and colonies with products showing the correct size of *GABRA3* cDNA were considered to indicate successful ligation. Minipreps from these colonies were prepared as detailed above. Afterwards, aliquots of extracted plasmids (250 ng pIRES α_3 DNA) were double-digested using 1 µl each of XhoI and BamHI, as well as 4 µl FastDigest Green buffer (Thermo Fisher) mixed with H_2O and left at 37°C for 15 minutes. Then, the products

were again checked on a 1% agarose gel. After that confirmation, minipreps were sent for sequencing using the primers listed in *Table 5*. The final pIRES-*GABRA3*-AcGFP is highlighted in *Figure 5*. Mutagenesis in the newly cloned construct was performed analogously to the aforementioned experiments (see section 2.3.2).

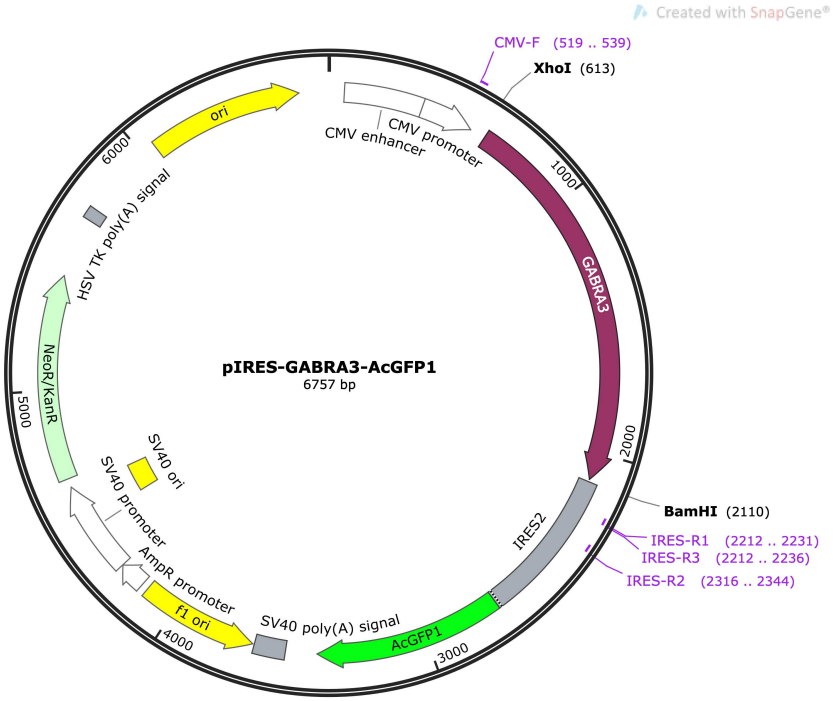

Figure 5. Map of the finished cloned pIRES-*GABRA3*-AcGFP plasmid. Restriction enzyme and primer binding sites are once again highlighted.

3.2.7 Maxiprep of all constructs

In order to increase the amount of DNA used for the cell experiments, a Maxiprep was performed. For this, the Genopure Plasmid Maxi Kit (Roche) was used. First, bacteria stock was added to 5 mL LB medium and its respective antibiotic and left at 37 °C for about 4 hours. That preculture was then mixed with another 250 mL of LB medium and its adequate dosage of antibiotic. The main culture was set into a shaking incubator of

37 °C over night - like this, the bacteria could grow.

The next day, the cultures were spinned at 5,000 g and 4 °C for 10 minutes, discarding the remaining supernatant medium. Using 12 mL Suspension Buffer + RNAse, the pellets were resuspended. Then, 12 mL Lysis Buffer was added to the falcon. The falcon was inverted and incubated for 2-3 min at RT to break up the bacterias' cell membrane. During this step, the filter system was prepared: 6 mL Equilibration Buffer was put onto the filter. 12 mL chilled Neutralization Buffer was mixed into the the falcon filled with the plasmid and Lysis Buffer and put on ice for 5 minutes, before putting the falcon onto the prepared filter. This step was performed to extract the bacterial debris from the desired DNA product. The next step was to further purify the obtained product. 16 mL of Wash Buffer were added twice, discarding the liquid that had flown through. Finally, pre-warmed Elution Buffer was pipetted onto the filter. Using a fresh falcon tube, the liquid was collected. 11 mL of isopropanol was mixed with the eluted DNA and inverted for purification purposes, then spinned at 8,500 rpm at 4 °C for 1h. The supernatant was discarded and 4 mL chilled 70% EtOH was added for the falcon to be spinned at 12,000 g at 4 °C for another 30 minutes. This served further purification purposes. Once again, the liquid was discarded. This time, the remaining pellet was left to air-dry. Finally, the pellet was resuspended in 100 µl sterile water. The concentration was measured using Nanodrop.

3.3 Expression in *Xenopus laevis* oocytes

3.3.1 DNA linearisation

As the goal was to inject translatable RNA into the oocytes to record the Cl^- currents passing through the GABA receptor, pcDNA3.1 vectors of the respective subunits of $GABA_A$ (α_3 WT and variants, β_2, and γ_2) needed to be linearised. To obtain this, 10 µg of plasmid was used, mixed with 5 µl of CutSmart buffer (New England BioLabs; NEB) and 1 µl of BamHI restriction enzyme (NEB), as the plasmid used contained a corresponding recognition site (cut site: G/GATCC; see *Figure 5*). Topped off to a total volume of 20 µl with H_2O, the tube was digested at 37°C for 2 hours. After that, the concentration was measured using Nanodrop (Thermo Fisher) and used for RNA synthesis. In the meantime before further usage, it was stored at -20°C.

3.3.2 RNA preparation

The linearised DNA as detailed above was used for transcription into RNA. 1 µg of the desired subunit DNA was mixed with 1 µl rNTPs, 1 µl RNAse Inhibitor, 2.5 µl 10 x buffer, 2.5 µl Cap-Analogon, and 1 µl T7 polymerase. DEPC H_2O was added to receive a total volume of 27 µl per tube. After quickly centrifuging, the reaction was incubated at 37°C for 2 hours. Then, 10 U of DNAse (1 µl) was added and left for 30 minutes to remove the template. All reagents were purchased from Roche.

3.3.3 RNA purification

Following the transcription process, the RNA was purified using a Phenol/Chloroform extraction method. This was performed by adding 50 µl of DEPC H_2O and 150 µl of

Phenol/Chloroform to the aforementioned RNA, transferring it to a Phase Lock Gel Eppendorf tube. This was spinned for 2 minutes at 14.000 g, then 100 µl of Isochloroform were added and again the tube was centrifuged as before. The supernatant was transferred to a new tube, mixed briefly with 1/10 the volume of sodium acetate (3M, pH = 5.3) and 3 x the volume of 100 % Ethanol. After having been left at -80°C overnight, the tube was centrifuged once more at 4°C for 15 minutes, discarding the liquid after that. Then, 300 µl of 70 % Ethanol were added, centrifuging and discarding the supernatant as described in the step immediately before. The remaining pellet was diluted in 20 µl of DEPC H_2O after having been left to dry. Like this, we obtained a purified injectable RNA. The concentration was measured via Nanodrop (Thermo Fisher) and checked on a 1 % agarose gel with gel electrophoresis. The finished product was stored at -80°C for best conservation.

3.3.4 Preparation of *Xenopus leavis* oocytes

The oocytes were delivered from Dr. Lohmann Diaclean GmbH - EcoCyte Bioscience, Dortmund (defolliculated and ready for injection) or the Animal Physiology, Tübingen University. Whenever the oocytes were provided by the Animal Physiology, they were treated with 1 mg/ml collagenase in OR-2 solution (consisting of 82.5 mM NaCl, 2.5 mM KCl, 1.0 mM $MgCl_2$, 5 mM Hepes buffer, pH = 7.6) and rotated for two hours before further use. After washing the individual oocytes with Barth's solution (containing in mM: 88 NaCl, 2.4 $NaHCO_3$, 1 KCl, 0.41 $CaCl_2$, 0.82 $MgSO_4$ and 5 Tris/HCl, pH 7.4 adjusted using NaOH), the oocytes were distributed evenly in wells filled with 200 µl of Barth's solution and 50 µg/ml Gentamicin. They were then left to rest for an hour before injection.

3.3.5 Injection of *Xenopus leavis* oocytes

Injections were performed using the automated injection system Roboinject (Multi Channel Systems MCS GmbH, Reutlingen) and the prepared RNA. α_3, β_2, and γ_2 subunits of the $GABA_A$ receptor were injected in a relation of 1:1:2. The RNA mix had a concentration of 2 µg/µl, using 70 nl for each oocyte. Whenever heterozygous conditions were going to be recorded, the relation was 1:1:1:2, so the same concentration of the mutation as wildtype of the α_3 RNA was injected into the oocyte.

After injection, the oocytes were kept at 18°C for 4 days in order for the RNA to be translated into proteins and for the expressed subunits to assemble into pentameric receptors in the oocyte membrane. For each variant, homozygous and heterozygous conditions were tested. Although the heterozygous conditions are not physiological, as the gene is located on Chromosome X, they were recorded for quality control purposes. Furthermore, H_2O-injected oocytes were recorded as a control condition.

3.3.6 Recordings using Robocyte

The 96-well plate containing the injected and incubated oocytes were placed into the Robocyte2 (Multi Channel Systems MCS GmbH, Reutlingen). It is a fully automated system that is able to do electrophysiological recordings in oocytes. After insertion of the plate into the robot, the Robocyte2 was calibrated in relation to its electrodes. As two-electrode automated voltage clamp was applied, the current was sampled at 1 kHz at a -70 mV holding potential in the membrane. The two intracellular pipettes containing the current and voltage electrode from the measuring head were filled with 1 M KCl and 1.5 M KAc, showing a resistance of 0.3 - 1.8 MΩ. Adding to that, the

preformed measuring head contains one current drain, one voltage and current electrode with respective references. The washing solution was ND96 (see *Table 6*). This solution was also used for the GABA solutions (1 mM, 300 µM, 100 µM, 30 µM, 10 µM, 3 µM, and 1 µM) that were subsequently applied to the oocytes by making use of the two perfusion outlets. First, an expression test with 1 mM of GABA solution (dissolved in ND96) was performed to find out whether the cell was emitting currents at all. Afterwards, the previously mentioned concentrations of GABA dissolved in ND96 solutions were applied to obtain the respective current responses of the cell. The purpose of that was to calculate a dose response curve of the cell and consequently the variant (Leisgen et al., 2007). After each application of GABA, a washing process took place to ensure a common baseline for each step.

Chemical Ingredient	Concentration [mM]
NaCl	9.35
KCl	0.2
$CaCl_2$	0.18
$MgCl_2$	0.2
HEPES	0.5

Table 6. ND96 solution components used as washing solution as well as dilutions during the oocyte experiments. The solution was adjusted to pH = 7.5.

Figure 6. The fully automated Roboocyte2 system as used in the experiments described (Multi Channel Systems MCS GmbH, Reutlingen).

3.3.7 Oocyte data analysis

Robocyte+ (Multi Channel Systems MCS GmbH, Reutlingen) was used to visualise the recorded currents. The software was used for the recording protocols and data analysis. The minima of the resulting currents were used in data analysis. Subsequently, dose response curves and resulting amplitudes were acquired.

A general response to the application of 1 mM GABA was analysed, normalised to the mean of the WT current of that day to ensure comparability of the various batches of cells.

To establish a dose response curve, the recorded currents corresponding to the various applied GABA concentrations were normalised to the maximum current of the recorded cell. According to the following formula:

$$Y = min + \frac{max - min}{1 + 10^{(log_{EC50} - X) * nH}}$$

an exponential curve to fit the normalised current (response; Y) was defined, with EC_{50} as the concentration where 50 $\%$ of the maximum current was achieved and nH as Hill coefficient. Statistical analysis was performed using Graphpad Prism 7 (GraphPad Software). A Kruskal-Wallis-test (non-parametric ANOVA on ranks) with Dunn post-hoc test were performed to test the significance of observed differences in normalized responses (corrected for multiple testing using a Bonferroni procedure). The significance of the differences in dose response curve fit parameters (EC_{50}, coefficient) were assessed using their 95 $\%$ confidence intervals (absence of overlap vs. the WT was considered to indicate significance), as well as a non-parametric ANOVA of the EC_{50}.

3.4 Recordings in murine neurons

3.4.1 Cell culture

Cover slips were prepared in a 24-well plate in advance, using 0.1 mg/ml of Poly-D-Lysin -hydrobromide (PDL) for each well. They were left overnight at 5°C, then the PDL was taken off and the wells were treated with UV light for 10 minutes and stored at 5°C sealed until needed for plating the neurons.

The cultures originated from terminated C57/Bl6N mice at embryonic stage of E17.5. The cells were prepared on cover slips covered with DMEM medium (Gibco) at 37°C.

They were washed with HBSS three times and then treated with 0.25 % Trypsin, letting the cells incubate at 37 °C for 14 minutes. Then, DMEM was used to wash another three times. Adding 1 ml of DMEM, the cells were filtered through a 0.45 micron filter and separated. Having counted the cells, around 70 000 - 80 000 were plated onto each well and incubated at 37°C. After 4 hours, the media was changed to Neurobasal medium and changed again every 3 to 4 days in order to nourish the cells properly. The neurons were stored inside a humidified CO_2 incubator at 37°C.

At DIV3 (3 days in vitro), the neurons were transfected using 1 µg of DNA and a mix of 4 µl Optifect Transfection Reagent with 100 µl Optimem (Thermo Fisher). Optifect was added to Optimem and incubated for 5 minutes. Following that, the DNA was added and left again for 20 minutes at room temperature before being distributed among the wells containing hippocampal/cortical neurons on cover slips. After 4 hours, the media were changed to 500 µl NB medium (Gibco) per well. 24-48 hours later the transfection was checked under fluorescent light microscope and starting from that moment, the cultures were being patched during a timeframe of one until up to 14 days.

3.4.2 Electrophysiological recordings

The currents were recorded from transfected cells using whole cell patch-clamp method in voltage clamp mode, . The successfully transfected neurons were visualised under fluorescent green light, as they were expressing GFP. For that, an air-suspended table with a Faraday cage served as the optimal surface and electric isolation for the setup with the Vert.A1 Axio microscope (Zeiss; see *Figure 7*). This setup facilitated the acquisition of current recordings. Glass pipettes with filament from Science Products (0.86 x 1.50 x 80 mm) were pulled using a Sutter P97 (Sutter Instrument Company) with a

resistance between 2 and 5 MΩ. They were filled with intracellular solution at pH = 7.4 and 300 mosm/kg (see *Table 7*) and the cell gently sucked in to record its currents. Whole cell patch clamp method was used, where negative pressure was applied to the cell in order to perforate the cell membrane. In turn, the cell was sealed with the purpose of recording and amplifying its currents. The extracellular solution, into which the cover slip containing the neurons was transferred and the reference bath electrode was placed, consisted of 136 mM NaCl, 2 mM KCl, 3 mM $MgCl_2$, 2 mM $CaCl_2$, 10 mM HEPES, and 20 mM Glucose (pH = 7.4, 310 mosm/kg). The Axopatch 200B amplifier (Axon Instruments) and Axon Digidata 1550B digitizer (Axon Instruments) were utilised to obtain the recordings. The holding potential was selected to be -70 mV and the filter was at 10 000 Hz. Compensation was usually at 85 %. The recording protocol sampled the currents for 5 minutes, after the cell had reached a Gigaseal, was opened, and properly compensated. Spontaneous inhibitory postsynaptic currents (sIPSCs) and miniature inhibitory postsynaptic currents (mIPSCs) were recorded. For sIPSCs, 10 µM NBQX and 100 µM AP-V were added to the extracellular solution to block AMPA- and Kainate channels. In order to attain mIPSCs, 1 µM of TTX, blocking voltage gated sodium channels, was added to the aforementioned solution.

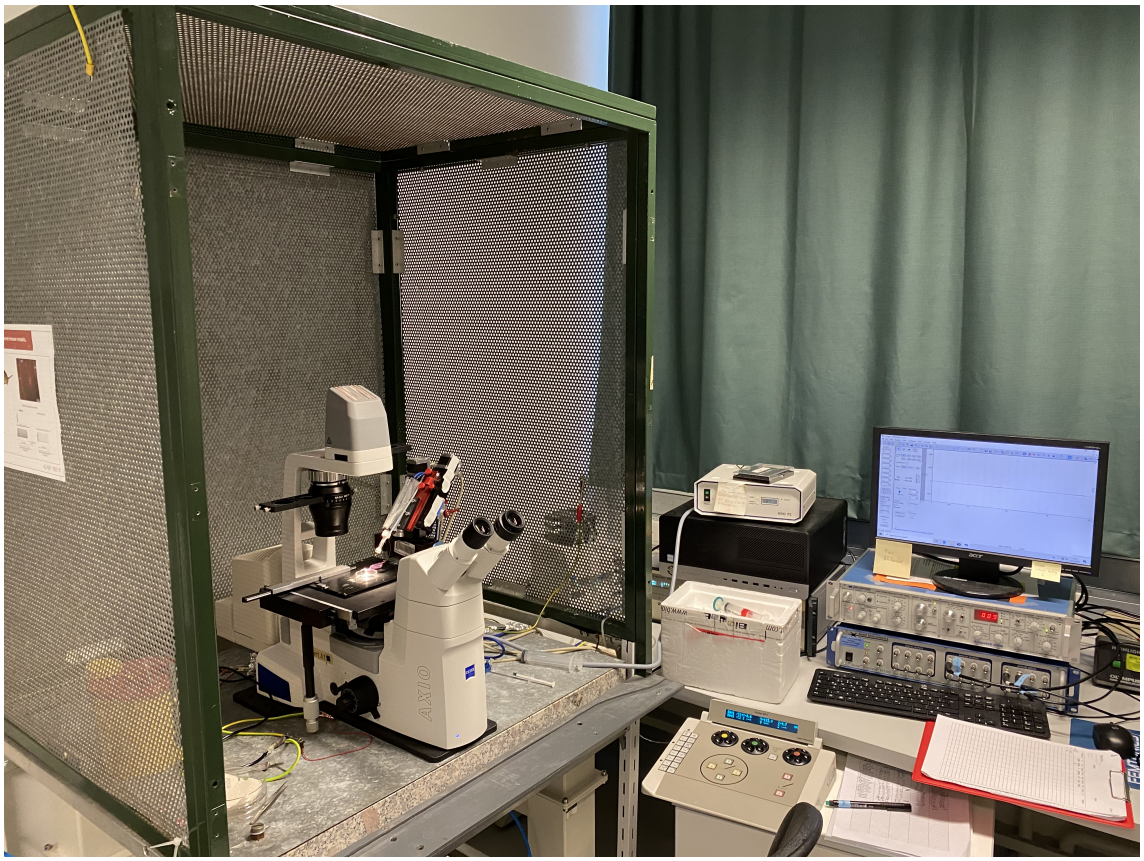

Figure 7. Setup used for patching of murine neurons using the whole cell patch clamp method including digitiser, amplifyer, and microscope.

Substance	Concentration [mM]
CsCl	130
HEPES	10
EGTA	10
ATP-Mg	4
GTP-Na	0.4
Biocytin	0.2%

Table 7. Intracellular solution used for patch clamping in neurons.

3.4.3 Analysis of neuronal data

Spontaneous inhibitory post synaptic currents (sIPSCs) and miniature inhibitory post synaptic currents (mIPSCs) were analysed using Clampfit 11 software (Molecular Devices). The obtained amplitudes, current frequencies, and decay tau were transferred to Microsoft Excel (Microsoft). Their means including SEM were calculated in Graphpad Prism 7. The data were tested for normal distribution. For not naturally distributed data, values were compared to each other using Kruskal-Wallis tests (non-parametric ANOVA).

3.4.4 Fixation of cultured cells

After having patched the cover slips, they were washed with PBS (Gibco) before being treated with Formaldehyde mixed with PBS in a 1:10 relation for 10 minutes. Afterwards, PBS was applied for washing purposes for another three times and stored at 4°C between 1 and 3 weeks to prepare them for stainings.

3.4.5 Immunofluorescence staining and imaging

The aim was to illustrate the patched cells with their expressed GABA $\alpha 3$ subunits using immunofluorescence. Cells were washed with a 0.1 % Triton solution in PBS three times and incubated for five minutes each. Then, Streptavidin (at 647 nm) diluted 1:1000 in PBS was applied onto the cover slip and incubated for 2 hours while being slightly rocked. This was done to facilitate the identification of the Biocytin-filled patched cells. As the intracellular solution that was used during patch clamp contained Biocytin, one could identify these same cells by having Streptavidin react with Biocytin. Their 647

nm made it possible to visualise the Biocytin-filled cells under a fluorescent microscope. After incubation, the cells were washed three times with PBS. For each washing step, PBS was applied to the cover slips containing the neuronal cultures and left on a rocking surface for five minutes. Subsequently, the cultures were treated with blottoTBS (4 % nonfat milk powder and 0.1 % Triton diluted in 10 mM Trishydroxymethylaminomethane, pH = 8.0) for an hour at 4°C. At a 1:1000 relation, the first antibody (Anti-*GABRA3*, Sigma-Aldrich) was added to blottoTBS and left on the cells at 4°C overnight. The next morning, after having treated the cultures once more with TBS-Triton solution three times for five minutes each, the second antibody was applied. Anti-rabbit 568 nm was diluted 1:500 in blottoTBS and incubated at room temperature for 1.5 hours. Having been washed 3 times for 5 minutes with PBS -/- to get rid of the excess, the finished cover slips were mounted on microscope slides and treated with anti-fade mounting medium (including 4',6-Diamidin-2-phenylindol; DAPI), as well as sealed with nail polish for further use and inspection under a fluorescent microscope.

Using a Zeiss Apotome microscope, the stained cultured cells were displayed. GFP (at 568 nm) visualised the cells transfected with GABA α_3 subunit DNA (WT or variants), Streptavidin (647 nm) tagged the α_3 subunits, and the use of DAPI (500 nm) was to visualise the fixated cells.

4 Results

4.1 Characterisation of clinical cases and oocyte experiments

4.1.1 Genetic evaluation of the variants

To get a first sense of the possible pathogenicity of the variants, an analysis of its deleteriousness, constraint, and conservation was performed as detailed above, including minor allele frequency. The results are detailed in *Table 8*. One can infer that the variant D115E is highly deleterious, changing a highly conserved and constrained site. The position affected by Y243C was conserved as determined by GERP++ and its Para-Z-Score. It was predicted to be deleterious, and as D115E, disrupted a highly constrained sire as determined by MPC and MTR. The V309L variant showed similar results as Y243C on all scales. The position affected by the last variant, S393I, which was only predicted to be deleterious by CADD, did not appear to be well-conserved and not constraint when considering its MTR or MPC results. All variants did not appear in control populations as interpreted by their MAF, except for S393I.

Variant		MAF		
cDNA change	Amino Acid	gnomAD	Top-Med	DiscovEHR
c.345T>A	D115E	0	0	0
c.728A>G	Y243C	0	0	0
c. 925G>C	V309L	0	0	0
c.1178G>T	S393I	0	0	<0.001

Variant		Deleteriousness		
cDNA change	Amino Acid	CADD	PPh2	REVEL
c.345T>A	D115E	24.9	0.99	0.81
c.728A>G	Y243C	27.0	1.0	0.92
c. 925G>C	V309L	24.8	0.99	0.76
c.1178G>T	S393I	21.9	0.30	0.16

Variant		Conservation		Constraint	
cDNA change	Amino Acid	GERP++	Para-Z-Score	MTR	MPC
c.345T>A	D115E	4.23	1.29	0.63	2.56
c.728A>G	Y243C	5.38	0.79	0.30	2.91
c. 925G>C	V309L	4.98	0.04	0.55	2.59
c.1178G>T	S393I	1.33	-1.46	1.05	0.65

Table 8. MAF: Minor allele frequency. Deleterious: CADD $\geqslant$20; PPh2 $\geqslant$0.85; REVEL $\geqslant$0.50. Conserved: GERP++ $\geqslant$2; Para-Z-score $\geqslant$0. Highly constrained: MTR $\leqslant$0.565; MPC $\geqslant$2.

The variants were also investigated across different species and other $GABA_A$ receptor subtypes to approximate the importance of their location within the gene products. This was done to supplement the *in silico* predictions obtained from the scores as determined above. The amino acid sequences of the orthologs and paralogs respectively are detailed below in *Figures 8 & 9* (UniProt Consortium, 2021). Both the scores and the sequences underlined the conservation of D115E, Y243C, and V309L. Their high deleteriousness was also congruent with the obtained results. Therefore, the scores could be plausibly confirmed by studying the orthologs and paralogs below.

Human	105	VSDTDMEYTI D VFFRQTWHDE
Rhesus	105	VSDTDMEYTI D VFFRQTWHDE
Dog	105	VSDTDMEYTI D VFFRQTWHDE
Mouse	105	VSDTDMEYTI D VFFRQTWHDE
Chicken	86	VSDTDMEYTI D VFFRQSWRDE
X.tropicalis	157	VSDTDMEYTI D VFFRQSWLDE

Human	233	VAQDGSRLNQ Y DLLGHVVGTE
Rhesus	233	VAQDGSRLNQ Y DLLGHVVGTE
Dog	233	VAQDGSRLNQ Y DLLGHVVGTE
Mouse	233	VAQDGSRLNQ Y DLLGHVVGTE
Chicken	214	VAKGGSRLNQ Y DLLGHVVGTE
X.tropicalis	285	VAPDGSRLNQ Y DLLGVAVGTE

Human	299	LNRESVPART V FGVTTVLTMT
Rhesus	299	LNRESVPART V FGVTTVLTMT
Dog	299	LNRESVPART V FGVTTVLTMT
Mouse	299	LNRESVPART V FGVTTVLTMT
Chicken	280	LNRESVPART V FGVTTVLTMT
X.tropicalis	351	LNRESVPART V FGVTTVLTMT

Human	383	KTPAAPAKKT S TTFNIVGTTY
Rhesus	383	KTPAAPAKKT S TTFNIVGTTY
Dog	383	KTPAAPTKKT S TTFNIVGTTY
Mouse	383	KTPAAPTKK- N TTFNIVGTTY
Chicken	364	KEPVALVKKT N NTYNIVGTTY
X.tropicalis	435	KEPIILAKKS N TTYNIVGTTY

Figure 8. Orthologs across different species of D115, Y243, V309, S393 (from top to bottom) and their surrounding amino acids. All variants except for S393 were well-conserved across different species.

```
GABRA1    D90  VSDHDMEYTI D VFFRQSWKDE
GABRA2    D90  VSDTDMEYTI D VFFRQKWKDE
GABRA3    D115 VSDTDMEYTI D VFFRQTWHDE
GABRA4    D96  VSDVEMEYTM D VFFRQTWIDK
GABRA5    D97  VSDTEMEYTI D VFFRQSWKDE
GABRA6    D80  VSDVEMEYTM D VFFRQTWIDE

GABRA1    Y218 VAEDGSRLNQ Y DLLGQTVDSG
GABRA2    Y218 VAPDGSRLNQ Y DLLGQSIGKE
GABRA3    Y243 VAQDGSRLNQ Y DLLGHVVGTE
GABRA4    Y224 VPKESSSLVQ Y DLIGQTVSSE
GABRA5    Y225 VAEDGSRLNQ Y HLMGQTVGTE
GABRA6    Y208 VPEESSSLLQ Y DLIGQTVSSE

GABRA1    V284 LNRESVPART V FGVTTVLTMT
GABRA2    V284 LNRESVPART V FGVTTVLTMT
GABRA3    V309 LNRESVPART V FGVTTVLTMT
GABRA4    V290 INKESVPART V FGITTVLTMT
GABRA5    V291 LNRESVPART V FGVTTVLTMT
GABRA6    V274 INKESVPART V FGITTVLTMT

GABRA1    N365 KKVKDPLIKK N NTYAPTATSY
GABRA2    N364 KKEKASVMIQ N NAYAVAVANY
GABRA3    S393 KTPAAPAKKT S TTFNIVGTTY
GABRA4    A392 ANLNMRKRTN A LVHSESDVGN
GABRA5    T374 KKREVILNKS T NAFTTGKMSH
GABRA6    I360 SKATEPLEAE I VLHPDSKYHL
```

Figure 9. Amino acid differences within human paralogs of various GABA receptors and their equivalent sequence positions.

4.1.2 Acquired clinical data

A family with neurodevelopmental disorder expressed the D115E variant. Its segregation analysis was positive for α_3. The Y243C variant was present in a female patient with dysmorphisms, brain abnormalities, well controlled epileptic seizures, and moderate intellectual disability. The V309L variant was also present in female patient as a *de novo* mutation. S393I was discovered in a male patient.

4.1.3 Electrophysiological results in oocytes

For the functional analysis of the discovered variants to determine of their pathogenicity, current responses were recorded in *Xenpous laevis* oocytes. Representative traces (1 mM GABA application) are shown in *Figure 10*. The mean normalised response (± Standard Error of the Mean; SEM) to application of 1 mM GABA in cells injected with WT mRNA was 102.8 % (± 8.6 %; n = 41) whereas the average normalised response for the tested variants was as follows (± SEM): Y243C = 9.8 % (± 2.6 %; n = 12); D115E = 44.2 % (± 7.9 %; n = 16); S393I = 57.6 % (± 16.8 %; n = 10); V309L = 142.3 % (± 34.9 %; n = 14). Compared to the normalised WT amplitude (range = 13.6 - 232.3 %), Y243C had low responses (range: 0.8 % - 24.7 %). The responses in D115E recordings were slightly variable, although still lower than the WT (range: 0.2 % - 96.4 %). The responses for S393I ranged between 8.1 % and 179 % and V309L showed a range between 5.7 % and 472.9 %. A Kruskal-Wallis test confirmed that the differences in ranked normalised responses between these five groups (WT, 4 variants) were significant ($p < 0.0001$). Post-hoc significance testing for pairwise differences between the WT and each variant (Dunn test; Bonferroni correction) indicated a significant reduction in normalised responses for Y243C ($p < 0.0001$) and D115E ($p < 0.01$) but not S393I ($p = 0.0741$) or V309L ($p > 0.9999$; see *Figure 11*).

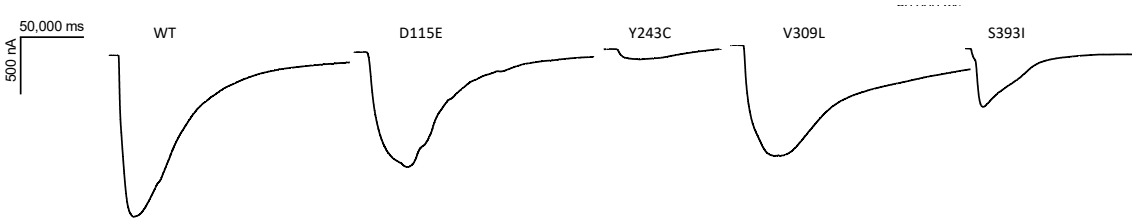

Figure 10. Representative GABA-evoked currents as recorded from oocytes injected with either WT or variant mRNA (D115E, Y243C, V309L, and S393I).

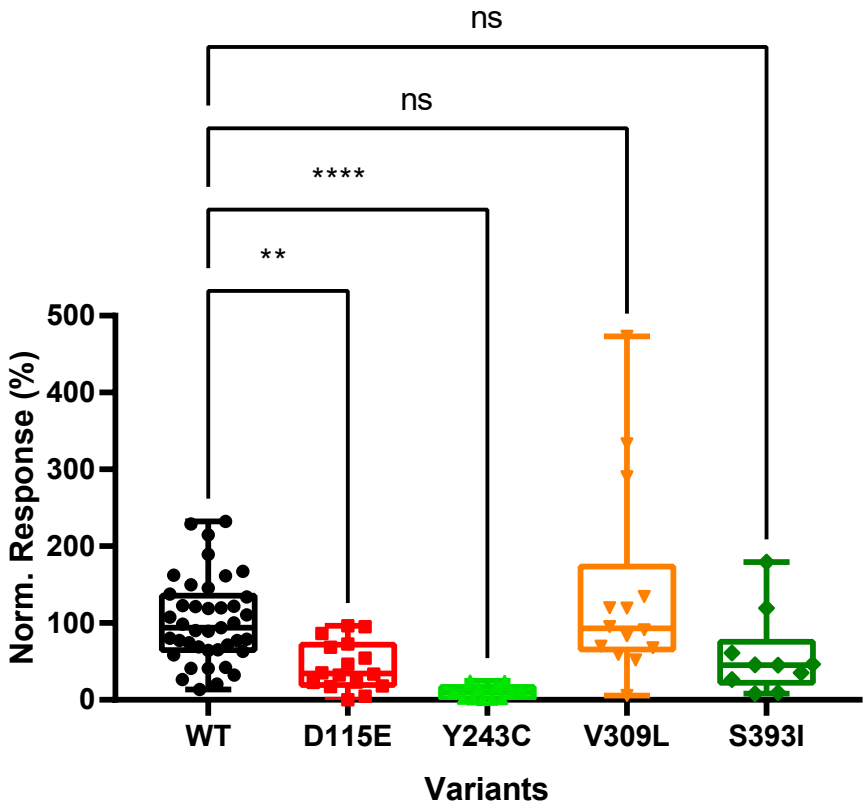

Figure 11. Boxplot of the normalised amplitudes of the average WT of each recording day. To calculate a normalised amplitude, the variant cell currents were divided by the mean of the WT on the respective recording day. Shown are pooled data from all recording days. Median and interquartile ranges (IQR) are shown for the WT as well as for each variant. Dots are individual normalised amplitudes. Minimum and maximum

currents mark the range of responses: WT median = 93.8 % (IQR = 64.8 - 135.7 %; n = 41), D115E median = 34.34 % (IQR = 19.3 - 71.8 %; n = 16), Y243C median = 9.2 % (IQR = 1.6 - 16.7 %; n = 12), V309L median = 93.0 % (IQR = 65.5 - 173.4 %; n = 14), S393I median = 45.3 % (IQR = 22.2 - 75.8 %; n = 10). The test used was a Kruskal-Wallis test.

To characterise the channel activity in response to GABA stimulation, the dose response curves of $\alpha_3\beta_2\gamma_2$ WT vs. variant expressions were calculated as shown in *Figure 12 A - E*. The EC_{50} Confidence Intervals (CI) are between 79.8 - 93.2 for the WT, 76.7 - 86.8 for D115E, 53.4 - 60.4 for Y243C, 30.0 - 42.2 for V309L, and S393I shows a CI between 94.6 - 116.2. Judging by the non overlapping of CIs for Y243C, V309L, and (vs. WT), one can infer a significant change (left shift in the case of V309L and Y243C, right-shift for S393I) compared to the WT dose response curve.

Comparing the EC_{50} values of the Y243C and V309L variant to the WT, they also showed significant differences using non-parametric statistical testing. They were at $p < 0.01$ and $p < 0.001$, respectively. The D115E, as well as the S393I variant did not differ significantly from the WT EC_{50} when performing a Kruskal-Wallis test.

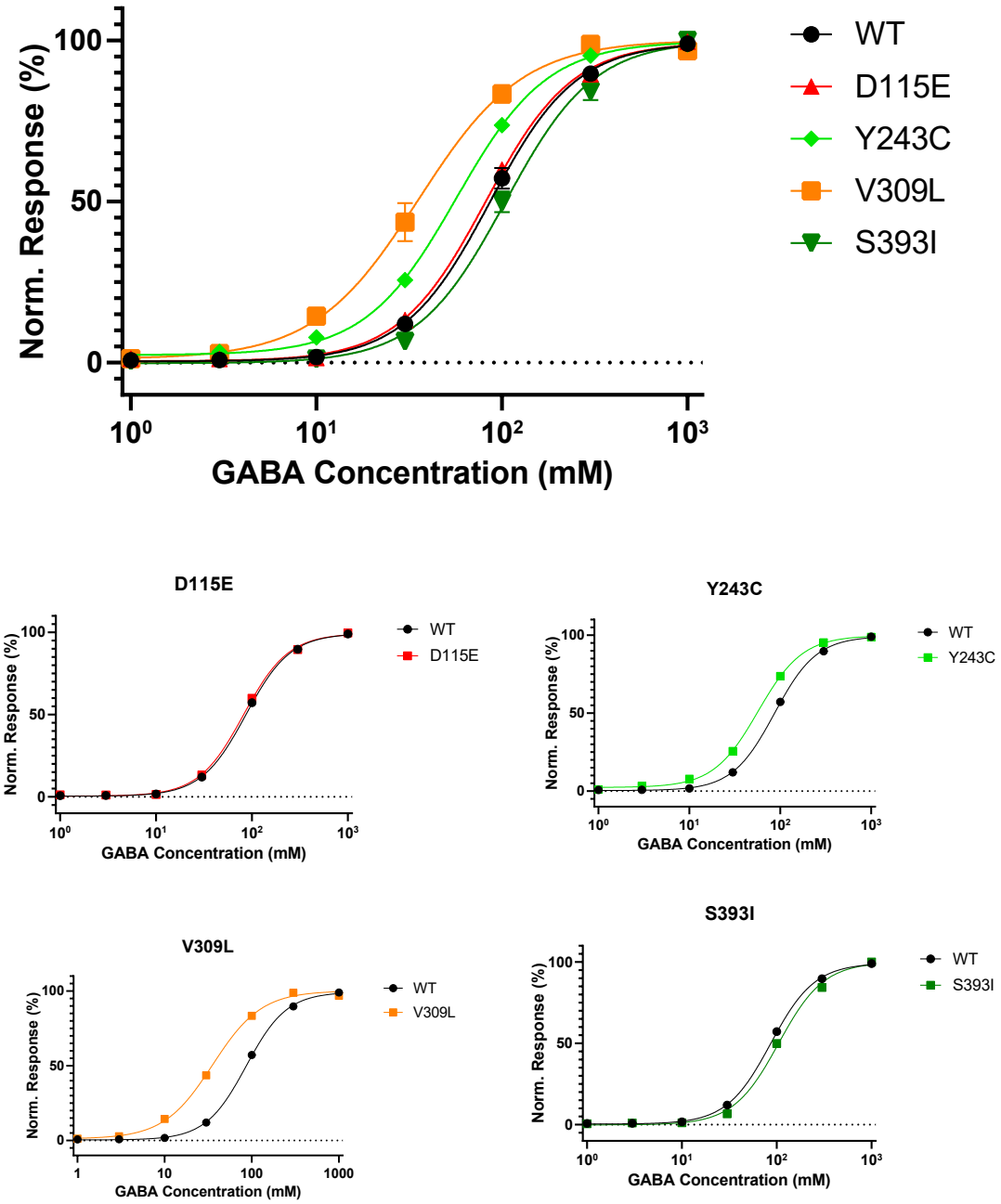

Figure 12 A - E. Dose response curves calculated using the various recorded currents of the respective conditions normalised to their own maximum current. For the WT condition n = 28 cells were recorded. n = 11 (D115E), n = 6 (Y243C), n = 6 (V309L), and n = 8 (S393I). The mean responses when applying 1 µM, 3 µM, 10 µM, 30 µM, 100 µM, 300 µm, and 1 mM GABA solution are shown as data points. B - E show each variant detailed individually as compared to the WT dose response curve.

Dose response cures were also calculated as current amplitudes of the variants compared to the average maximum WT response of the corresponding recording day. The results are shown below in *Figure 13*. The D115E variant showed a comparable dose response curse as the WT but had a decreased sensitivity when compared to its own maximum current response. In the case of the Y243C variant, a slight sensitisation could be inferred from the dose response curve. V309L had an increased sensitivity compared to the WT dose response curve over both conditions. The S393I variant stayed at the same tendency of a reduced sensitivity to GABA application.

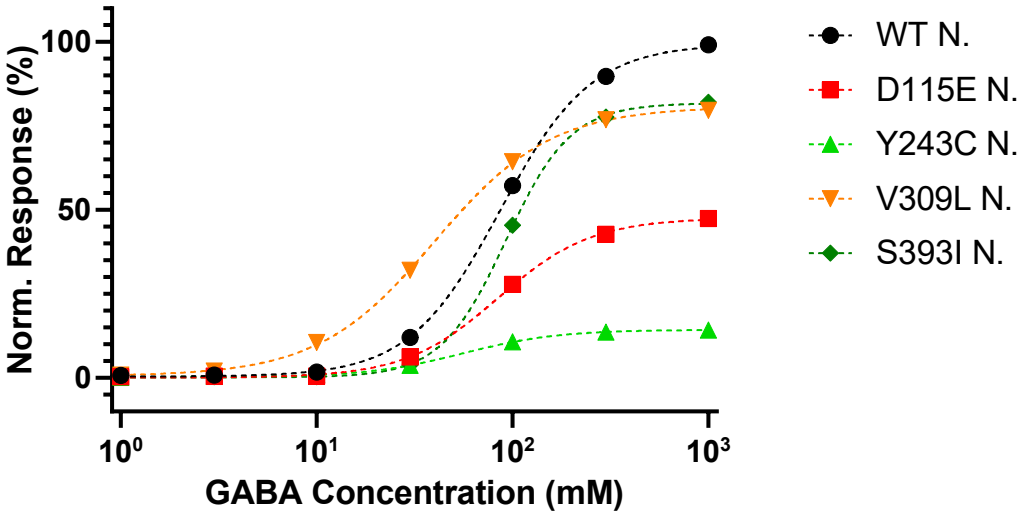

Figure 13. Dose response curves of the various variant recordings, normalised to the corresponding average maximum WT recording.

A few heterozygous cells were examined as well to have further insight into the electrophysiologcal changes. The results are shown in *Figure 14*. The mean recorded current amplitude relative to the average WT response of the day including SEM was at 77.2 ±

22.4 % for D115E, 112.7 ± 30.2 % in the case of Y243C, 306.9 ± 85.5 % for V309L, and 57.1 ± 20.2 % for the S393I variant. The average response of the WT is at 102.8 ± 8.6 %.

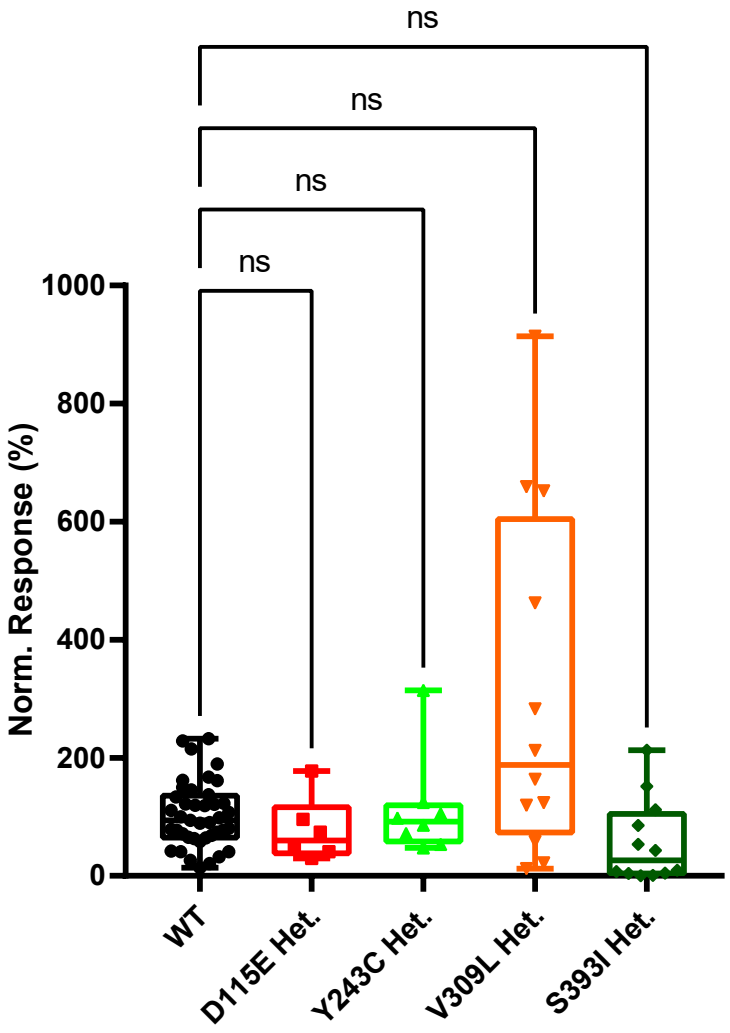

Figure 14. Averaged normalised amplitudes of heterozygous conditions with WTα_3, variant α_3, β_2, and γ_2 in a relation of 1:1:1:2. n = 41 (WT), n = 6 (D115E), n = 8 (Y243C), n = 12 (V309L), and n = 12 (S393I) were used. A Kruskal-Wallis test was performed and yielded non-significant results.

4.2 Neurons and imaging

4.2.1 Spontaneous inhibitory post synaptic currents

Spontaneous inhibitory currents were recorded, as shown in *Figure 15*. Mean amplitudes, frequencies, as well as the decay time were investigated.

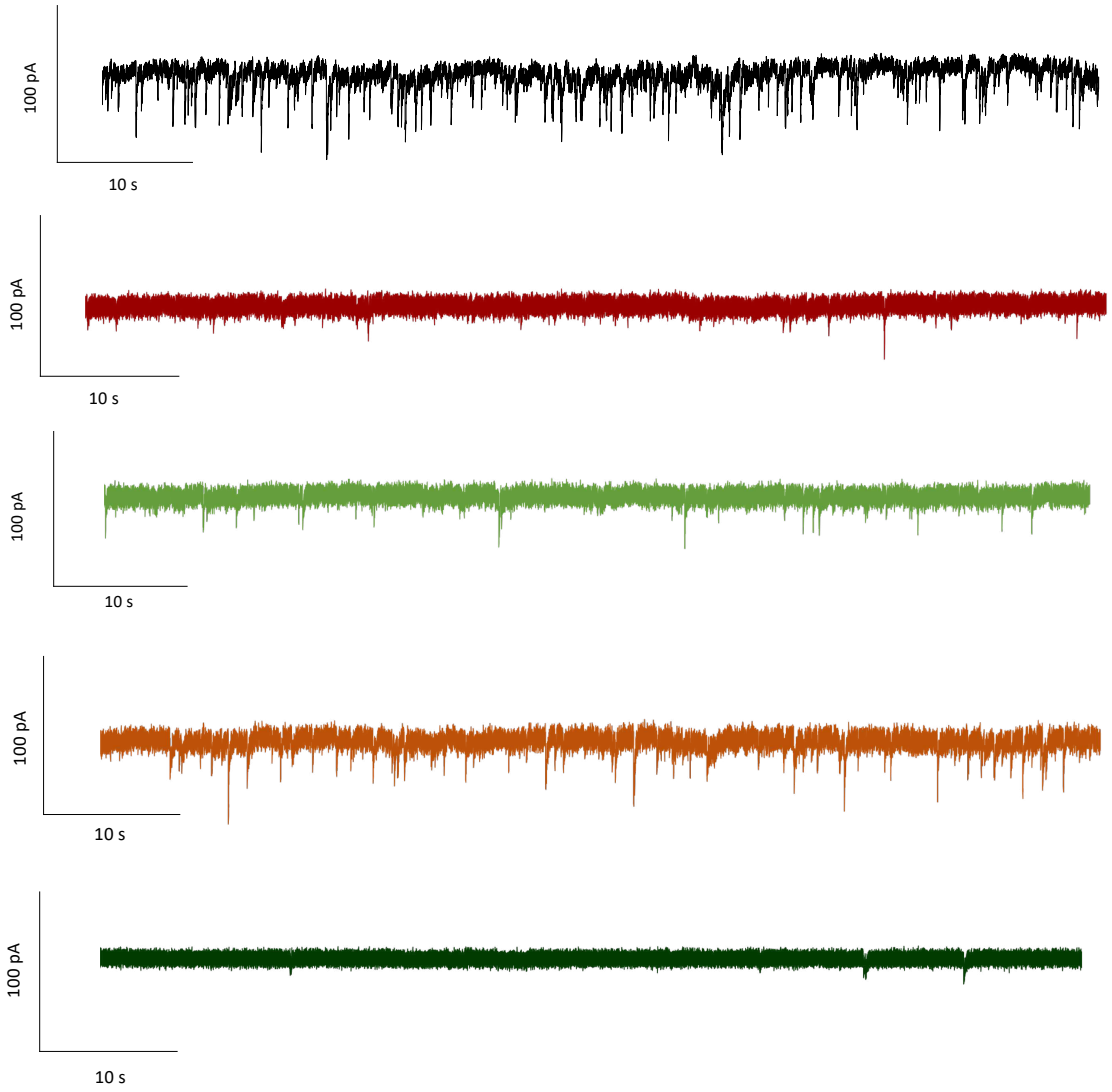

Figure 15 A - E. Representative currents recorded from neurons transfected with either WT or variant constructs.

When comparing the recorded sIPSC amplitudes, no change was discovered. WT current amplitudes were 28.6 ± 5.6 nA. D155E showed a mean amplitude of 23.8 ± 2.0 nA, Y243C 39.8 ± 5.6 nA, V309L 45.1 ± 11.9 nA, and S393I 31.5 ± 8.5 nA. The values listed are the arithmetic mean, as well as the corresponding standard error of the mean. Below, in *Figure 16*, the values including the results of the performed Kruskal-Wallis-Test are summarised.

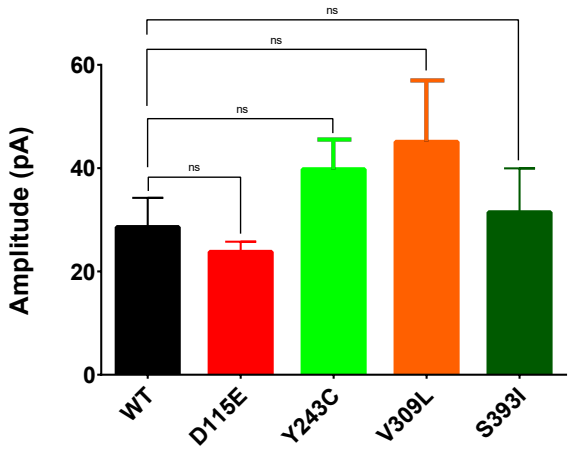

Figure 16. n = 7 WT cells, n = 3 D115E cells, n = 5 Y243C cells, n = 3 V309L cells, and n = 3 S393I cells were included into the analysis. Depicted are means ± SEMs, as well as a summary of the performed Kruskal-Wallis tests (ns: not significant). Exact results of the performed test are as follows: in comparison to the WT $p > 0.9999$ for D115E, $p = 0.6291$ in the case of Y243C, for V309L $p = 0.6060$, and $p > 0.9999$ as results of the performed analysis concerning the comparison in amplitudes.

In contrast, the sIPSC frequencies were significantly changed. Neurons transfected with the WT plasmid had a mean frequency of 1.35 ± 0.24 Hz, D115E 0.33 ± 0.09 Hz, Y243C 0.76 ± 0.27 Hz, V309L 0.50 ± 0.19 Hz, and S393I 0.26 ± 0.09 Hz. As the data was not normally distributed, the performed Kruskal-Wallis was significant for S393I compared to the WT with $p = 0.0206$. The summarised results are shown in *Figure 17*.

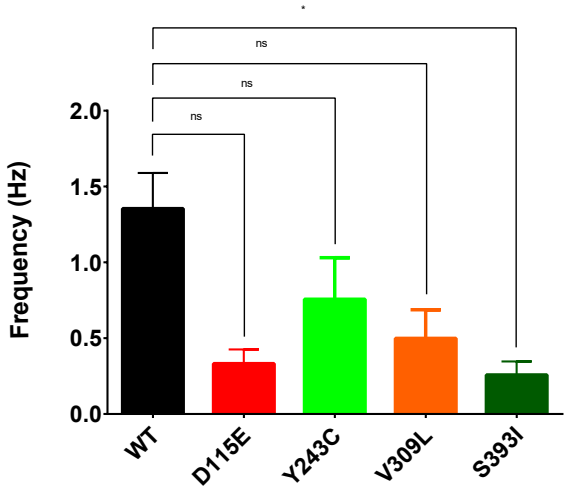

Figure 17. After performing a Kruskal-Wallis test (* $p < 0.05$; ns: not significant) comparing the WT to respective variants, D115E was at $p = 0.0712$, Y243C at $p = 0.4811$, V309L at $p = 0.2496$, and S393I at $p = 0.0206$ (*). n = 7 WT cells, n = 3 D115E cells, n = 5 Y243C cells, n = 3 V309L cells, and n = 3 S393I cells were used.

Next, the exponential time washout of the sIPSC decay was determined. The WT showed a mean tau of 63.2 ± 3.3 ms (arithmetic mean ± SEM), D115E 107.7 ± 8.2 ms, Y243C 60.5 ± 8.0 ms, V309L of 214.1 ± 78.1 ms. S393I was analysed to have a mean tau of 86.9 ± 9.6 ms. This time, D115E as well as V309L differed significantly from the WT condition, with $p = 0.0463$ for both variants when performing a Kruskal-Wallis test. The results are detailed in *Figure 18*.

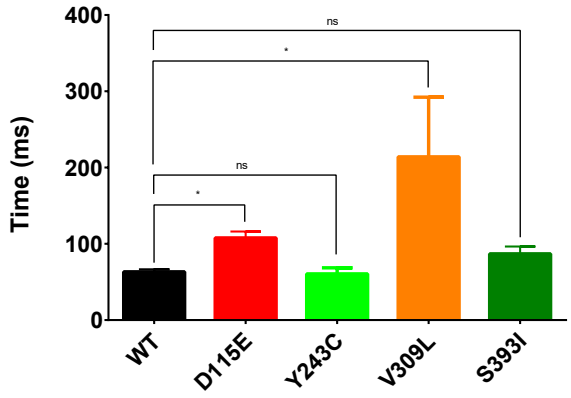

Figure 18. Decay time analysis of n = 7 WT cells, n = 3 D115E cells, n = 5 Y243C cells, n = 3 V309L cells, and n = 3 S393I cells. The Kruskal-Wallis test results are (* p < 0.05; ns: not significant): p(D115E) = 0.0463 (*), Y243C was at $p > 0.9999$, V309L was at $p = 0.0463$ (*), and S393I was at $p = 0.3811$ when compared to the WT.

4.2.2 Miniature inhibitory post synaptic currents

To record miniature inhibitory post synaptic currents, TTX was added to the extracellular solution from singular released synaptic vesicles. Data are shown as mean ± SEM.

In *Figure 19 A - E*, exemplary recorded currents are shown to illustrate the results further.

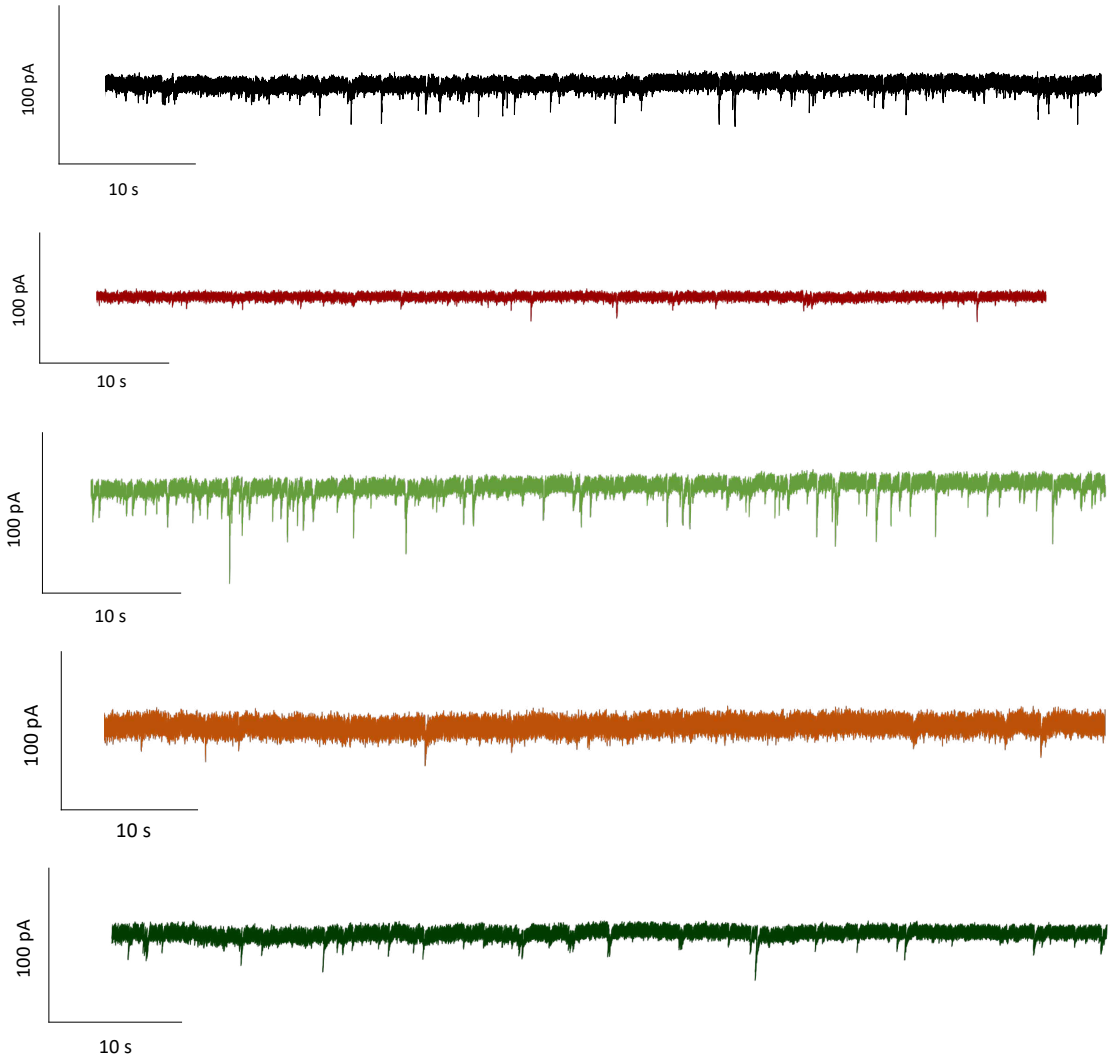

Figure 19 A - E. Representative traces of mIPSC recordings recorded from neurons transfected with either WT or variant α_3 $GABA_A$ receptor cDNA (D115E, Y243C, V309L, S393I).

The mean amplitude of the WT cells was at 23.9 $\pm$ 4.2 nA. On average, the D115E variant amplitude recordings were at 16.8 $\pm$ 1.1 nA, whereas Y243C was at 29.8 $\pm$ 5.0 nA. The V309L variant's amplitude was on average at 26.1 $\pm$ 9.8 nA, and S393I is at 31.5 $\pm$ 8.1 nA. None of these values showed a significant difference to the WT in the statistical analysis. The results are shown in *Figure 20*.

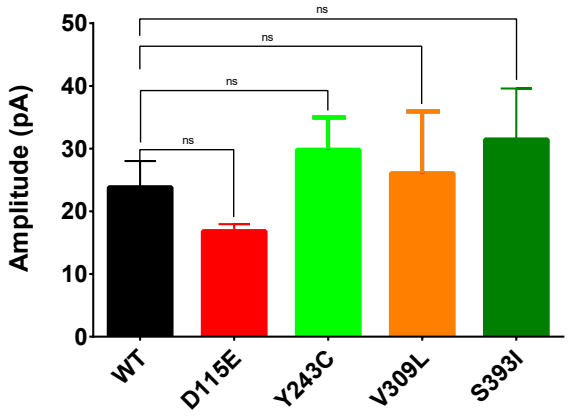

Figure 20. Mean + SEMs and amplitude in nA for n = 5 WT cells, n = 5 D115E cells, n = 4 Y243C cells, n = 3 V309L, and n = 4 S393I cells. The performed Kruskal-Wallis test comparing the variants to the average WT gave $p > 0.9999$, except for D115E, in which case $p = 0.3911$.

Furthermore, the frequency of the mIPSCs was analysed. Neurons transfected with WT cDNA had a mean frequency of 0.63 $\pm$ 0.20 Hz. The D115E variant was at a mean frequency of 0.33 $\pm$ 0.10 Hz and Y243C had an average frequency of 0.51 $\pm$ 0.20 Hz. V309L was calculated to have a rate of 0.35 $\pm$ 0.12 Hz. Finally, the S393I variant had a frequency of 0.416 $\pm$ 0.09 Hz. Considering the statistical test and grouped analysis, no variant differed significantly in their mean frequency in comparison to the WT. Once again, the averaged results are portrayed in *Figure 21*.

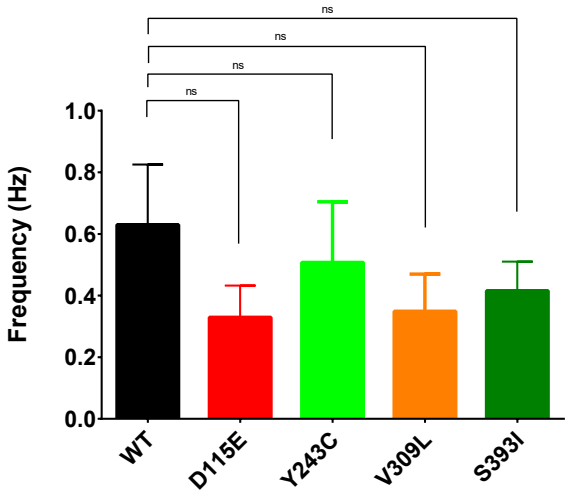

Figure 21. Mean frequency + SEM is given in Hz for n = 5 WT cells, n = 5 D115E cells, n = 4 Y243C cells, n = 3 V309L, and n = 4 S393I cells. For the D115E variant, $p = 0.5761$, Y243C was at $p > 0.9999$, V309L had a $p = 0.8949$, and S393I was at $p > 0.9999$ when comparing their frequencies to the WT in a Kruskal-Wallis test.

WT cells had an average decay tau of 66.0 ± 11.8 ms. The D115E variant was at 76.9 ± 13.9 ms, and the Y243C variant 72.1 ± 4.0 ms. The V309L variant had a mean tau of 122.5 ± 36.7 ms. Finally, the recorded S393I cells showed a mean tau of 58.0 ± 4.9 ms. None of these values were statistically significant in a grouped analysis when comparing the variants to the WT. In *Figure 22*, this information is visualised.

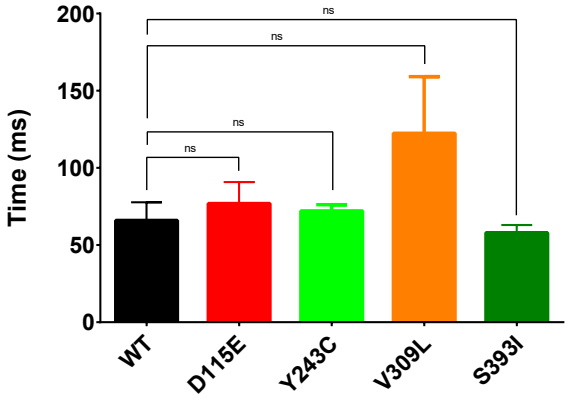

Figure 22. Mean values + SEM are depicted in ms. n = 5 WT cells, n = 5 D115E cells, n = 4 Y243C cells, n = 3 V309L, and n = 4 S393I cells were included in the statistical analysis. D115E, Y243C, and S393I were all at $p > 0.9999$. V309L showed a p-value of $p = 0.3085$ when performing a Kruskal-Wallis test, comparing the variants to the WT.

4.2.3 Immunostaining and imaging of transfected neurons

After having performed immunostainings on cells fixed with formaldehyde, they were imaged and investigated underneath the microscope. Representative cells of all transfected conditions are shown in *Figures 23 A - H*. This was done to verify the presence of α_3 in presumed $GABA_A$ receptors within the cell membrane, tracing the recorded postsynaptic currents to the effect of these variants.

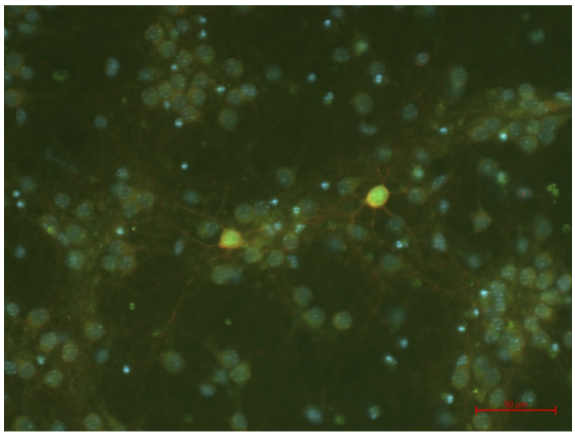

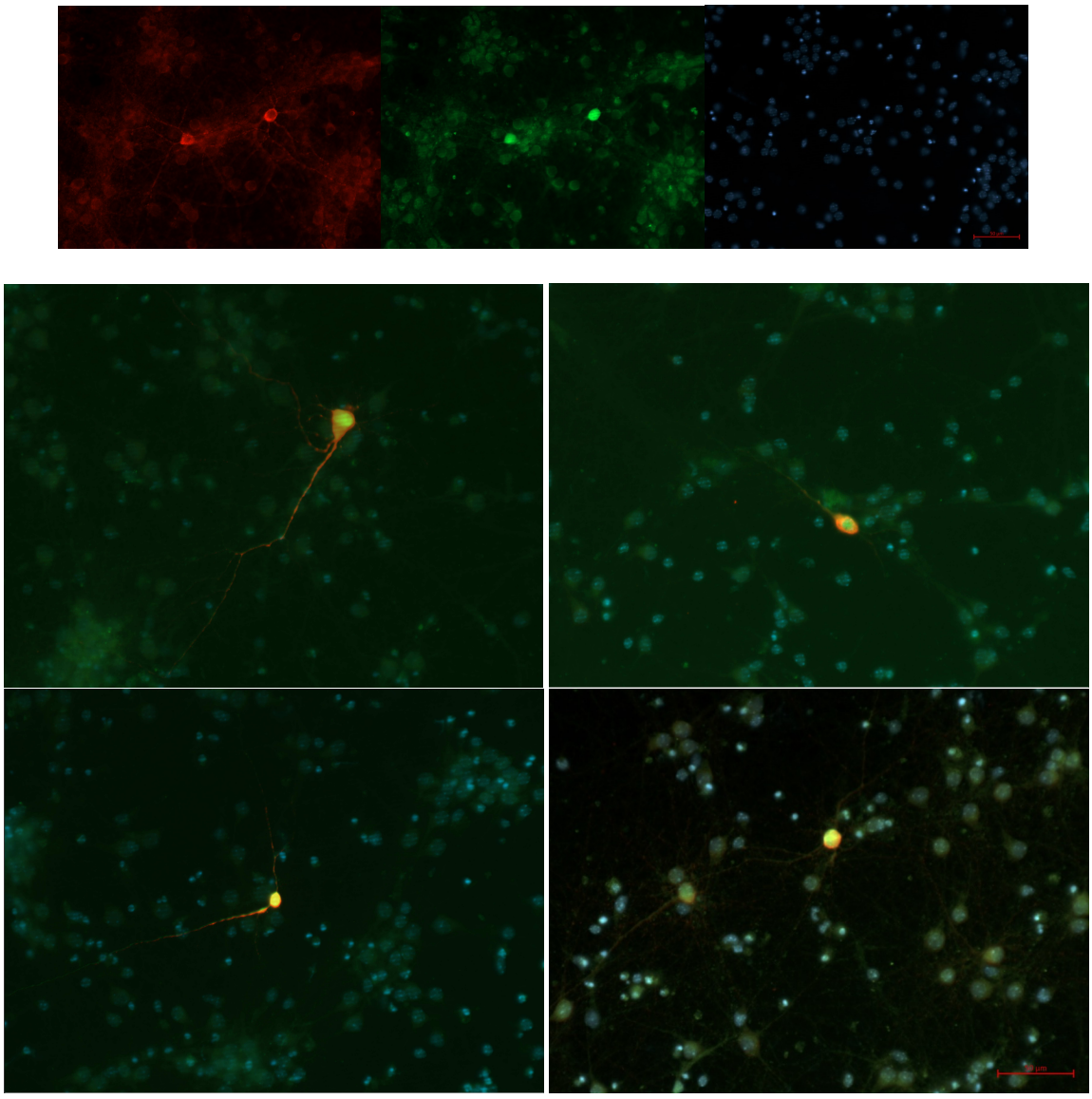

Figures 23 A - H. Overview of an exemplary patched WT neuron *(A)*. *B - D* show the same neurons with Anti-GABA-α_3, visualising the expressed receptors, GFP (shows that the cell has been transfected, as the cDNA construct contained GFP), and DAPI (fixed cells), respectively. Overviews of D115E, Y243C, V309L, and S393I cells are shown from top left to bottom right in *E - H*. Bars indicate 50 µm.

5 Discussion

5.1 Interpretation of results

5.1.1 Phenotypic severity of the variants related to their molecular analysis and electrophysiological recordings

The D115E variant showed significantly decreased anion current amplitudes in response to GABA compared to the WT in oocytes (see *Figure 11*). The GABA sensitivity was similar to the WT (see *Figure 12*), yielding an overall loss-of-function mechanism (see *Figure 13*). Recorded currents when expressing the heterozygous condition (see *Figure 14*), as well as the immunohistochemistry stainings done in neuronal cultures (see red staining in *Figure 19*) support the assumption that $GABA_A$ receptors were transported into the cell membranes. The pathogenicity of a malfunctioning receptor by expression of this variant is further supported by its localisation in the N-terminal extracellular domain near the GABA binding site, thus a functionally highly important region, as inferred by the homologous amino acid sequences in the α_1 subunit (Baumann et al., 2003). This is further supported by the fact that the affected residue is well conserved across different species and homologous amino acids in various $GABA_A$ subunits (see *Figures 8 and 9*). The previously described G47R and T166M variants of the $GABA_A$ receptor α_3 subunit are just like the D115E variant similar in their GABA sensitivity when compared to the WT, and they showed a decrease in overall GABA response, even though only T166M was statistically significant. The G47R variant was mainly clinically striking by the presence of ASD. T166M also manifested mostly with intellectual disability (Niturad et al., 2017). This relates to the family with the D115E variant, which has a neurodevelopmen-

tal disorder as a main phenotype. Furthermore, the electrophysiological characteristics within mutations of the N-terminal extracellular domain appear to be similar (decrease in mean overall response).

Regarding the obtained results in neurons, the sIPSCs recorded from neurons overexpressing the D115E variant showed a significantly accelerated decay, whereas the mean amplitude and frequency remained slightly reduced compared to the recorded cells overexpressing the WT (though not statistically significant). This implies that less GABA is released from the presynaptic cell. The oocyte findings would suggest a reduced frequency and/or amplitude when studying sIPSCs and mIPSCs ((Olsen & Sieghart, 2016)). The increase in decay time suggests altered kinetics, as previously observed in oocytes. The precise conclusion is left to be drawn because of the small sample size in neurons.

The oocyte experiments showed remarkable results for the Y243C variant which are in line with the previous oocyte study conducted by Niturad and colleagues (Niturad et al., 2017). Considering the cells expressing the variant to 1 mM of GABA solution, the response was highly significantly decreased (see *Figure 11*). The dose response curve showed a slight increase in GABA sensitivity when comparing it to the WT (see *Figure 12*). The normalised dose response curve showed a decreased anion dose response in response to GABA when compared to the maximum WT response (see *Figure 19*), indicating a predominant loss of function. Considering the conservation across paralogs and orthologs, the variant is well conserved (see *Figures 8 and 9*), supporting our findings that this missense variant significantly impairs receptor function. Furthermore, the amino acid is located in the first extracellular domain of the protein, containing the

signalling peptide. Again, the receptor appears in the membrane, as shown by the immunohistochemistry (see *Figure 19*). The conclusions drawn from the analysis of neurons transfected with either WT or variant cDNA point toward a decreased frequency and increased amplitude in sIPSCs/mIPSCs. Further recordings with a much larger number of recorded might be necessary to detect significant differences in recordings from neurons. If correlating these findings, one would normally infer a decreased frequency and amplitude for the recorded neurons (see (Olsen & Sieghart, 2016). From this variant, one can draw comparisons to the missense variant Q242L (Niturad et al., 2017), which has also shown significantly smaller overall oocyte currents related to the WT. Just like the variant next to it (our studied variant Y243C), it showed an increased GABA sensitivity, so a gain of function mechanism concerning GABA sensitivity might be of further pathogenic relevance ((Ahring et al., 2021)). Clinically, the variant also lead to moderate intellectual disability (even though it ranges from mild to severe), as well as facial abnormalities. Seizures were also present and treated with Valproate, among other antiseizure medications (Niturad et al., 2017), affecting the GABA equilibrium within the brain. Since the *GABRA3* gene is located on the X chromosome, one could infer that male patients are more severely affected clinically, as they have only one X chromosome. Concluding these observations, implications for the patients affected could be that the variant Y243C is indeed pathogenic. The female patient's symptoms can therefore be sensibly understood by her altered $GABA_A$ receptors containing α_3 subunits.

Even though the mean current response to 1 mM of GABA solution application seemed to be decreased in the S393I variant, it was not statistically significant (see *Figure 11*). The calculated dose response curve showed a significantly decreased sensitivity to GABA (see *Figure 12*). The normalised dose response curve showed decreased anion currents in response to the applied GABA solution (see *Figure 13*). Considering paralogs and orthologs (see *Figures 8 and 9*), the protein region is not very well conserved. Furthermore, the variant is located on an intracellular loop and might therefore not embody a great contribution to the described phenotype. The mother of the described male case also carried the variant but was not affected. The receptors were expressed in the membrane as visualised with immunohistochemistry (see *Figure 19*). A significant decrease in sIPSC frequency could be determined. One can support the findings in oocytes by the data recorded from neurons, pointing in the direction of reduced vesicular release of GABA (Pinheiro & Mulle, 2008). The decay time stayed approximately the same across sIPSCs as well as mIPSCs, and the decrease in frequency when comparing the variant to the WT was not observed for mIPSCs. The amplitudes did not show a change in either condition, implying a regular postsynaptic activation of receptors (Nusser et al., 1997). Therefore, the patient's symptoms can most likely not be fully explained by the electrophysiological characteristics of their S393I variant.

5.1.2 Loss of Function in *GABRA3*

Previous findings in *GABRA3* have been mainly associated with a decreased receptor function when variants were studied *in vitro*. This was determined by considering the overall current response of variant vs. WT cells. The electrophysiological properties were indicating that a loss of receptor function contributed to the respective clinical conditions.

Below, in *Table 9*, the receptor function finding is subsumed for the previously established pathogenic variants (Niturad et al., 2017).

Variant	Normalised max response	Dose response curve	dose response curve normalised to WT
G47R	reduced	comparable to WT DRC	decreased overall response
T166M	sig. reduced	comparable to WT DRC	decreased overall response
Q242L	sig. reduced	increased sensitivity	decreased overall response
T336M	sig. reduced	increased sensitivity	decreased overall response
Y474C	sig. reduced	increased sensitivity	decreased overall response

Table 9. Recorded electrophysiological properties in oocytes as described (Niturad et al., 2017). DRC: dose response curve; WT: wildtype

Overall, a reduced maximum response to GABA could be observed in all variants examined up to date when compared to the WT currents - the authors explained the phenotype partially by the degree of loss of function (Niturad et al., 2017). They inferred the loss of function by looking at the overall response. The characterised D115E variant showed similarities to T166M. The affected family's neurodevelopmental disorder was coherently explained by the oocytes' current response, relating to the degree of disease severity. Q242L could be compared to Y243C, as detailed in the above section - a loss of function in receptor function could be concluded. So far, no indication of an isolated gain of function has been described as a possible disease mechanism in *GABRA3*. In *GABRD*, however, only recently a possible gain of function mechanism has been described (Ahring et al., 2021).

5.2 Gain of function as a novel disease mechanism in *GABRA3*

Located in the second transmembrane domain (M2), V309L lines the ligand-gated receptor channel from the inside (Thompson et al., 2010). Investigating the GABA response in oocytes, it was on average not significantly decreased when compared to the WT (see *Figure 11*). The dose response curve lead to additional conclusions: The GABA sensitivity was highly increased as opposed to the WT curve (see *Figure 12*). Even normalised to the WT current, the overall response to GABA was increased (see *Figure 13*).

The decay time was also significantly increased in neuronal cultures transfected with the V309L variant when obtaining sIPSCs, meaning that the time for the recorded current to return to its baseline was prolonged. The decay was decelerated as compared to the WT which goes along with the oocyte findings, as the decrease in GABA sensitivity imply a longer desensitisation time. The amplitude of the sIPSCs was furthermore slightly increased, supporting the hypothesis of an increased postsynaptic activation. Yet the variability of the obtained amplitudes was quite large; that could be why the finding has not been proven to be significant as of now. The frequency was also not significantly decreased. mIPSCs showed similar tendencies, yet none were very prominent. In transfected neurons using V309L variant cDNA, $GABA_A$ receptors containing α_3 were expressed in the surface membrane, as shown in the respective immunohistochemistry assay (see *Figure 19*).

We conclude that the channel yielded an increased overall activity. The exact implications of that finding are yet to be determined. This is the first time a gain of function mechanism in a *GABRA3* variant has been linked to epileptic symptoms.

5.2.1 Gain of function variants in GABA$_A$

A gain of function variant appears to be counterintuitive at first sight, considering GABA as the main inhibitory neurotransmitter within the brain. Logically, seizures might not be induced when the inhibition of postsynaptic synapses are increased. As established in the introduction, GABA serves several functions in different stages of development, and is much more complex than just an inhibitory neurotransmitter. Tonic and phasic inhibition and their purpose need to be considered when evaluating the meaning of a gain of function variant, like V309L, for that matter.

To gain a better sense for this, it is important to consider other variants in GABA$_A$ subunits that have been described so far. Recently, the gain of function variant A322V was discovered in *GABRA1*. The increased sensitivity of the formed receptor was interpreted by recording currents from HEK cells (Steudle et al., 2020). The patient in question presented refractory seizures, and neurodevelopmental delay with dysmorphic facial features. The V284A variant of *GABRA2* was characterised similarly, where an increased GABA sensitivity could be observed in HEK cells, just as the V309L variant in *GABRA3* (Maljevic, Keren, et al., 2019). The phenotype was characterised to be absences and clonic seizures, as well as ocular revulsion with severe cognitive impairment and developmental delay. The *de novo* V294L variant in the α_5 subunit of GABA$_A$ receptors was also studied in HEK cells, with the result of an increased GABA sensitivity (Butler et al., 2018). However, the overall response to GABA was decreased. In that study, the decreased current response *in vitro* is traced back to increased desensitisation of the receptor. The amino acid position is near the V309L in α_3, also being a change from Valine to Leucine.

The phenotypes of neurodevelopmental disorders and generalised epilepsy within families and *de novo* mutations within *GABRD* could also be traced back to variant subunits which were shown to be overly active compared to their WT (Ahring et al., 2021). The variants within *GABRD* in question were located at P257L, L260V, and T291I, showing increased overall currents and and increased sensitivity, inferring from their dose response curve.

The β_3 subunit also contained several pathogenic variants that could be considered to increase receptor activity when studied *in vitro* (Absalom et al., 2022). *De novo* mutations were examined in *X. laevis* oocytes for that experiment after Vigabitrine had not been successful in treating the recurring seizures of the patients. Rather, an extreme reaction to the medication was observed, leading to the hypothesis that an increased receptor function of some sort could be responsible for the phenotype (Absalom et al., 2020). The mutations were located at E77K and T287I within the subunit. The patients showed epileptic encephalopathy with refractory spasms (Kothur et al., 2018) and developmental delay, dysmorphic features with varying kinds of seizures as part of an epileptic encephalopathy (Papandreou et al., 2016), respectively. The patients in question had an accentuated response to anti-seizure drugs enhancing the effect of GABA. That finding underlines the importance of selection of suitable treatment for patients. Not only is it advantageous to ascertain the kind of genetic variant. It is also important to know about the electrophysiological properties when matching appropriate therapeutic options to the genetic background of the phenotypes.

5.3 The decay of sIPSCs

Previously discovered findings for γ_2 variants showed significant differences in the time it takes until the recorded negative peak current returns to the baseline current (Eugène et al., 2007). The frequency and amplitude did not change when expressing variants within neuronal cultures. However, only mIPSCs were recorded in the γ_2 study. Two variants were studied that had previously shown a decrease in overall response when studied in oocytes with GABA application (Eugène et al., 2007). The K289M variant, which showed a more rapid deactivation as opposed to the WT, is located in the second extracellular domain, whereas R43Q, not being significant in kinetic alterations, is located at the N-terminus (Eugène et al., 2007).

In α_3's V309L and D115E sIPSCs, tau is significantly increased. This implies a prolonged time of recorded current. This could be either due to a gain of function - enriching the oocyte findings in the V309L variant. According to previous models, an accelerated decay should decrease the obtained amplitudes (Poncer et al., 1996). A slight decrease is observable in D115E, and an increase is present in V309L, as would be expected. To validate these findings, however, the amount of cells recorded needs to be increased.

S393I showed a significantly reduced frequency in sIPSCs which is interpreted as a reduction in GABA release from the presynaptic cell. Even though in oocyte experiments, S393I shows no significant difference in current response compared to the WT, it may still be the case that the presynaptic release of GABA is changed through altered receptors at postsynaptic sites. As established, feedback loops are part of synaptic adjustments (Jacob et al., 2008), making that mechanism plausible.

One needs to remark on the overall number of recorded neurons: the variability within

the cultured cells was very high, which is why the number of cells should be increased to further support our findings.

5.4 Possible underlying molecular mechanisms

Mechanisms such as protein stability, 3D formation, and receptor trafficking were discovered to be altered in *GABR* pathways (Macdonald et al., 2010). As for the *GABRA3* variants, one can infer that the α_3 subunits are present in the surface membrane. This implies a receptor function deficit, which needs to be studied further. Post translational phosphorylation and alteration might be impaired when editing the variant after translation (Jacob et al., 2008). Another possible mechanism is decreased protein stability and increased degradation, especially for variants located in transmembrane domains (Krampfl et al., 2005)

The established gain of function mechanism in the V309L variant could be due to increased extrasynaptic activation, as it is supposed for *GABRD* variants (Ahring et al., 2021).

5.5 Clinical implications

For the identified loss of function α_3 variants D115E and perhaps Y243C, benzodiazepines, phenobarbital, or valproate could be tried as possible treatments for the patients. These substances, used to treat seizures or used as sedatives, affect GABA homeostasis, increasing its inhibiting effect (Czapiński et al., 2005). Consequently, a decreased postsynaptic response would be enhanced, perhaps approaching physiological synaptic conditions. However, one should carefully consider the severe side effects before

starting treatment.

In case of V309L, medications used to block the ion channel could be tried to relieve affected individuals. Drugs such as flumazenil could be tried (Johnston, 2013). As for the previously described α_2 variant V284A, the patient affected was treated with phenytoin and sodium valproate (Maljevic, Keren, et al., 2019). In the case of α_5 gain of function variants, patients treated with phenobarbital and benzodiazepines reacted with an aggravation of seizures (Butler et al., 2018). A study in patients with β_3 variants showed hypersensitivity to Vigabatrin (Absalom et al., 2020), which could also aggravate the condition in our α_3 patients carrying the V309L variant, as Vigabatrin affects GABAergic neurons. It is therefore important to consider that some anti seizure medication might worsen the presented symptoms. This stresses the need to further explore molecular mechanisms in the pathogenesis of diseases, for example using a knock-in mouse model, as this study does not suffice for clear therapeutic implications. In order to find the treatment most suitable for the patient, knowing about the functional consequences of the variants is imperative. For example, variants within the voltage-gated sodium channel encoded on the *KCNA2* gene can successfully be treated in patients carrying a gain of function variant with 4-aminopyridine, a K+ blocker ((Oyrer et al., 2018)).

One approach for treatment that is still at its infancy and earliest stages would be gene therapy. In the case of another X chromosome related neurodevelopmental disorder with seizures, a proof of principle in treating mice has been successful (Gao et al., 2020). Knockout mice with deviations in cyclin-dependent kinase-like 5 (*CDKL5*) were studied in this case. An application of the corrected gene in adeno-associated viral vectors during prenatal development lead to higher expression of the WT. Moreover, recent

work has shown that postnatal expression of Cdkl5 in mice with CDKL5 Deficiency Disorder corrects the behavioral disturbances (i.e., the disease is reversible) suggesting a wide therapeutic window (Terzic et al., 2021), suggesting a possible future approach also to similarly affected genes, such as *GABRA3*.

5.6 Limitations

Concerning the oocyte experiments, the interpretation of results is insofar limited that they do not present a physiological environment and leave no room for conclusions in that regard.

When studying the variants in neurons, one needs to consider that neuronal cortical cultures contain a multitude of cell types. As α_3 is not well expressed within the hippocampus - which also consists of a variety of cell types - we did not opt for such cultures. Additionally, the amount of neurons recorded was quite small; future studies would need a larger sample size to support or contradict the established tendencies.

5.7 Strengths

The conducted study in oocytes is in line with previous findings, enhancing that *GABRA3* is a gene associated to epileptic seizures and neurodevelopmental disorders. It is the first of its kind to express α_3 in murine neurons, contributing to a more physiological understanding and modeling of the conditions. Even though the obtained results are not coherent in every case, the artificial oocyte data is enriched by a larger perspective. *GABRA3* is now associated to leading to pathological conditions in the scenario of a loss of function. The novel disease mechanism of gain of function for α_3 containing $GABA_A$

receptors was established.

5.8 Future work yet to be conducted

Further experiments concerning the tonic inhibition in neurons by applying PTX to the neuronal cultures and comparing these results to non-blocked recordings would enlarge the correlation between the results on molecular receptor function in oocytes and data obtained from the neuronal recordings.

Furthermore, a response to medications such as benzodiazepines or the new GABA-ergic drug cenobamate would be interesting to investigate, as the treatment implication resulting from these findings could benefit the affected individuals.

Another aspect to look into further is to clearly discern between developing neurons and already formed networks. As the transfection reagent were applied while the networks were still forming *in vitro*, there is no conclusion to reach about established connections. In order to reach further insight, one could try electroporation *in utero* to study the effect of the variants within brain slices, or study variants in knock-in mouse models.

The immunohistochemistry images taken (see *Figure 19*) could additionally used to quantify receptor expression in the cell membrane. For now, one can only infer for certain that α_3 subunits were expressed. Such is one way of approaching the molecular level of discerning whether it is a question of altered receptor function, formation, or transportation to the cell membrane. For that, an N-terminal tag with GFP of our gene would be suitable, enabling differentiation between naturally occurring subunits in the cell membrane and variants being expressed and incorporated. However, tagging might alter the protein 3D structure, possibly influencing receptor formation.

5.9 Concluding remarks

Two variants showed an overall loss of function by showing a collective reduction in current response to GABA, D115E and Y243C. D115E showed an accelerated decay of IPSCs when studied in neurons. These results may explain the clinical phenotype by mechanism of disinhibition. S393I, leading to a milder condition, yielded less certain results, supporting a correlation between genotype and phenotype. The variant led to fewer inhibitory post synaptic currents recorded in our preliminary experiments. The receptor function properties are influenced by the variants. As GABA binds to the α subunit (Baumann et al., 2003), it is plausible that a mutation within the corresponding *GABRA3* gene alters its properties and ability to bind GABA. In contrast, V309L showed a gain of function mechanism with increased GABA sensitivity of mutant receptors and an increase in decay time of IPSCs in transfected neurons. This is a new mechanism of the receptor and it is not yet evident how it leads to seizures.

6 Summary

Novel *GABRA3* variants with clinical phenotypes varying between neurodevelopmental disorders and epilepsy were investigated *in vitro* and characterised on an electrophysiological level. Mutagenesis was done in plasmids and *Xenopus laevis* oocytes as well as murine neuron cultures were used as expression systems. Two-electrode automated voltage-clamp was applied for the oocytes, whereas spontaneous inhibitory postsynaptic currents (sIPSCs) and miniature inhibitory postsynaptic currents (mIPSCs) were obtained by performing whole cell voltage clamp recordings in neurons. Additionally, immunohistochemical stainings were executed. The variants D115E and Y243C showed a decreased overall response to GABA application in oocytes. The S393I variant showed no significant difference in oocytes when compared to the wildtype. Recorded currents from neurons showed significant increased decay time in the D115E (sIPSCs and mIPSCs) and V309L (sIPSCs) variant, as well as decreased frequency in the S393I variant (sIPSCs), corresponding to the oocyte findings. This suggests a possible α_3 containing $GABA_A$ receptor impairment, affecting receptor sensitivity to GABA, as well as altered receptor function and kinetics. The D115E and Y243C variants were interpreted as a pathogenic loss of function variant judging from the reduced response to GABA, as well as decreased amplitude and frequency in sIPSCs and partially in mIPSCs. S393I was most likely not pathogenic. The V309L variant showed a pronounced increased GABA sensitivity in oocytes, leading to the establishing of gain of function variants as a new disease mechanism in *GABRA3*. The electrophysiological characterisation supplied possible explanations for the presented clinical conditions, implying the need for treatment adjustment tailored to the respective variants.

7 Zusammenfassung

Neuartige Varianten im *GABRA3* Gen mit unterschiedlichen klinischen Phänotypen wurden auf ihre elektrophysiologischen Eigenschaften hin charakterisiert, um die neurologischen Entwicklungsstörungen und Epilepsien dahingehend *in vitro* zu erklären. Mutagenese wurde in Plasmiden durchgeführt. *Xenopus laevis* Oozyten sowie Mausneurone wurden als Expressionssysteme gewählt. Ein automatisiertes zwei-Elektroden-Spannungs-Klemmen-System wurde verwendet, um die GABA-Ströme aus Oozyten zu messen. sIPSCs und mIPSCs wurden von Neuronen abgeleitet. In diesen Zellen wurden ebenfalls immunhistochemische Färbungen durchgeführt. Die Varianten D115E und Y243C zeigten in den Oozytenversuchen reduzierte Ströme auf GABA-Stimulation hin. Die S393I Variante zeigte keinen Unterschied in Oozyten im Vergleich zum Wildtyp. Aufgezeichnete Ströme von Neuronen zeigten eine signifikant verlängerte Decay-Zeit in den Varianten D115E (sIPSCs und mIPSCs) und V309L (sIPSCs) sowie eine verringerte Frequenz in der Variante S393I (sIPSCs), was mit den Ergebnissen in den Oozyten einhergeht im Sinne eines Funktionsverlusts oder einer -beeinträchtigung des α_3-haltigen $GABA_A$-Rezeptors. Die Varianten D115E und Y243C wurden aufgrund der verminderten Reaktion auf GABA sowie der verringerten Amplitude und Frequenz bei sIPSCs und teilweise bei mIPSCs als pathogene Funktionsverlustvariante interpretiert. S393I war höchstwahrscheinlich nicht pathogen. Die V309L-Variante zeigte eine ausgeprägte erhöhte GABA-Empfindlichkeit in Oozyten, was zur Etablierung von Gain-of-Function-Varianten als neuem Krankheitsmechanismus bei *GABRA3* führte. Diese elektrophysiologische Charakterisierung unterstützt die Hypothese, dass die Varianten zur vorliegenden Klinik beitragen, was die Anpassung medikamentöser Behandlungsmaßnahmen zur Folge hat.

8 References

Absalom, N., Liao, V., Johannesen, K., et al. (2022). Gain-of-function and loss-of-function *GABRB3* variants lead to distinct clinical phenotypes in patients with developmental and epileptic encephalopathies. *Nature Communications*, *13*(1). doi: https://doi.org/10.1038/s41467-022-29280-x

Absalom, N., Liao, V., Kothur, et al. (2020). Gain-of-function *GABRB3* variants identified in vigabatrin-hypersensitive epileptic encephalopathies. *Brain Communications*, *2*(2). doi: https://doi.org/10.1093/braincomms/fcaa162

Adzhubei, I., Schmidt, S., Peshkin, L., et al. (2010). A method and server for predicting damaging missense mutations. *Nature Methods*, *7*(4), 248 - 249. doi: https://doi.org/10.1038/nmeth0410-248

Ahring, P., Liao, V., Gardella, E., et al. (2021). Gain-of-function variants in *GABRD* reveal a novel pathway for neurodevelopmental disorders and epilepsy. *Brain*. doi: https://doi.org/10.1093/brain/awab391

Baulac, S., Huberfeld, G., Gourfinkel-An, I., et al. (2001). First genetic evidence of $GABA_A$ receptor dysfunction in epilepsy: a mutation in the γ_2-subunit gene. *Nature Genetics*, *28*, 46 - 48. doi: https://doi.org/10.1038/ng0501-46

Baumann, S., Baur, R., & Sigel, E. (2003). Individual properties of the two functional agonist sites in $GABA_A$ receptors. *Journal of Neuroscience*, *23*(35), 11158 - 11166. doi: https://doi.org/10.1523/JNEUROSCI.23-35-11158.2003

Behuet, S., Cremer, J., Cremer, M., Palomero-Gallagher, N., Zilles, K., & Amunts, K. (2019). Developmental changes of glutamate and GABA receptor densities in wistar rats. *Frontiers in Neuroanatomy*, *13*. doi: https://doi.org/10.3389/fnana.2019.00100

Ben-Ari, Y. (2002). Excitatory actions of GABA during development: The nature of the nurture. *Nature Reviews Neuroscience.*, *3*, 728 – 739. doi: https://doi.org/10.1038/nrn920

Bromfield, E., Cavazos, J., & Sirven, J. (2006). Chapter 1, basic mechanisms underlying seizures and epilepsy. *An Introduction to Epilepsy [Internet]*. Retrieved from `https://www.ncbi.nlm.nih.gov/books/NBK2510/`

Butler, K., Moody, O., Schuler, E., et al. (2018). De novo variants in *GABRA2* and *GABRA5* alter receptor function and contribute to early-onset epilepsy. *Brain.*, *141*(8), 2392 - 2405. doi: https://doi.org/10.1093/brain/awy171

Buxbaum, J., Silverman, J., Smith, C., et al. (2002). Association between a *GABRB3* polymorphism and autism. *Molecular Psychiatry*, *7*(3), 311 - 316. doi: https://doi.org/0.1038/sj.mp.4001011

Christian, C., Herbert, A., Holt, R., et al. (2013). Endogenous positive allosteric

modulation of GABA$_A$ receptors by diazepam binding inhibitor. *Neuron*, *78*(6), 1063 - 1074. doi: https://doi.org/10.1016/j.neuron.2013.04.026

Cossette, P., Liu, L., Brisebois, K., et al. (2002). Mutation of *GABRA1* in an autosomal dominant form of juvenile myoclonic epilepsy. *Nature Genetics*, *31*, 184 – 189. doi: https://doi.org/10.1038/ng885

Czapiński, P., Blaszczyk, B., & SJ, C. (2005). Mechanisms of action of antiepileptic drugs. *Current Topics in Medical Chemistry*, *5*(1), 3 - 14. doi: https://doi.org/10.2174/1568026053386962

Davydov, E., Goode, D., Sirota, M., Cooper, G., Sidow, A., & Batzoglou, S. (2010). Identifying a high fraction of the human genome to be under selective constraint using GERP++. *PLoS computational biology*, *6*(12). doi: https://doi.org/10.1371/journal.pcbi.1001025

DeLorey, T., Handforth, A., Anagnostaras, S., et al. (1998). Mice lacking the β_3 subunit of the GABA$_A$ receptor have the epilepsy phenotype and many of the behavioral characteristics of angelman syndrome. *Journal of Neuroscience*, *18*(20), 8505 - 8514. doi: https://doi.org/10.1523/JNEUROSCI.18-20-08505.1998

Dewey, F., Murray, M., Overton, J., et al. (2016). Distribution and clinical impact of functional variants in 50,726 whole-exome sequences from the DiscovEHR study. *Science*, *354*(6319). doi: https://doi.org/10.1126/science.aaf6814

El Achkar, C., Harrer, M., Smith, L., et al. (2021). Characterization of the *GABRB2*-associated neurodevelopmental disorders. *Annals of Neurology*, *89*(3), 573 - 586. doi: https://doi.org/10.1002/ana.25985

Epi25. (2019). Ultra-rare genetic variation in the epilepsies: A whole-exome sequencing study of 17,606 individuals. *The American Journal of Human Genetics*, *105*(2), 267 - 282. doi: https://doi.org/10.1016/j.ajhg.2019.05.020

Epi4K Consortium, & Epilepsy Phenome/Genome Project. (2013). *De novo* mutations in epileptic encephalopathies. *Nature*, *501*(7466), 217 – 221. doi: https://doi.org/10.1038/nature12439

Essrich, C., Lorez, M., Benson, J., Fritschy, J.-M., & Lüscher, B. (1998). Postsynaptic clustering of major GABA$_A$ receptor subtypes requires the γ_2 subunit and gephyrin. *Nature Neuroscience*, *1*, 563 – 571. doi: https://doi.org/10.1038/2798

Eugène, E., Depienne, C., Baulac, S., et al. (2007). GABA$_A$ receptor γ_2 subunit mutations linked to human epileptic syndromes differentially affect phasic and tonic inhibition. *Journal of Neuroscience*, *27*(51), 14108 - 14116. doi: https://doi.org/10.1523/JNEUROSCI.2618-07.2007

Farrant, M., & Nusser, Z. (2005). Variations on an inhibitory theme: Phasic and tonic activation of GABA$_A$ receptors. *Nature Reviews Neuroscience*, *6*, 215 – 229. doi:

https://doi.org/10.1038/nrn1625

Fisher, R., Acevedo, C., Arzimanoglou, A., et al. (2014). ILAE official report: A practical clinical definition of epilepsy. *Epilepsia*, *55*(4), 475 - 482. doi: https://doi.org/10.1111/epi.12550

Fisher, R., Cross, J., French, J., et al. (2017). Operational classification of seizure types by the international league against epilepsy: Position paper of the ILAE commission for classification and terminology. *Epilepsia*, *58*, 522 - 530. doi: https://doi.org/10.1111/epi.13670

Fritschy, J., Benke, D., Mertens, S., Oertel, W., Bachi, T., & Möhler, H. (1992). Five subtypes of type a gamma-aminobutyric acid receptors identified in neurons by double and triple immunofluorescence staining with subunit-specific antibodies. *Proceedings of the National Academy of Sciences*, *89*(15), 6726 - 6730. doi: https://doi.org/10.1073/pnas.89.15.6726

Fritschy, J., & Mohler, H. (1995). $GABA_A$-receptor heterogeneity in the adult rat brain: Differential regional and cellular distribution of seven major subunits. *Journal of Comparative Neurology*, *359*(1), 154 - 194. doi: https://doi.org/10.1002/cne.903590111

Fritschy, J., & Panzanelli, P. (2014). $GABA_A$ receptors and plasticity of inhibitory neurotransmission in the central nervous system. *European Journal of Neuroscience*, *39*, 1845 - 1865. doi: https://doi.org/10.1111/ejn.12534

Gao, Y., Irvine, E., Eleftheriadou, I., et al. (2020). Gene replacement ameliorates deficits in mouse and human models of cyclin-dependent kinase-like 5 disorder. *Brain*, *143*(3), 811 – 832. doi: https://doi.org/10.1093/brain/awaa028

Harkin, L., Bowser, D., Dibbens, L., et al. (2002). Truncation of the $GABA_A$-receptor γ_2 subunit in a family with generalized epilepsy with febrile seizures plus. *The American Journal of Human Genetics*, *70*(2), 530 - 536. doi: https://doi.org/10.1086/338710

Hutcheon, B., Fritschy, J., & Poulter, M. (2004). Organization of $GABA_A$ receptor α-subunit clustering in the developing rat neocortex and hippocampus. *European Journal of Neuroscience*, *19*, 2475 - 2487. doi: https://doi.org/10.1111/j.0953-816X.2004.03349.x

Ioannidis, N., Rothstein, J., Pejaver, V., et al. (2016). REVEL: an ensemble method for predicting the pathogenicity of rare missense variants. *The American Journal of Human Genetics*, *99*(4), 877 - 885. doi: https://doi.org/10.1016/j.ajhg.2016.08.016

Jacob, T., Moss, S., & Jurd, R. (2008). $GABA_A$ receptor trafficking and its role in the dynamic modulation of neuronal inhibition. *Nature Reviews Neuroscience*, *9*, 331

– 343. doi: https://doi.org/10.1038/nrn2370

Johnston, G. (2013). Advantages of an antagonist: bicuculline and other GABA antagonists. *British Journal of Pharmacology*, *169*(2), 328 – 336. doi: https://doi.org/10.1111/bph.12127

Kang, J., & Barnes, G. (2013). A common susceptibility factor of both autism and epilepsy: Functional deficiency of $GABA_A$ receptors. *Journal of Autism and Developmental Disorders*, *43*, 68 - 79. doi: https://doi.org/10.1007/s10803-012-1543-7

Kang, J., & Macdonald, R. (2009). Making sense of nonsense $GABA_A$ receptor mutations associated with genetic epilepsies. *Trends in Molecular Medicine*, *15*(9), 430 - 438. doi: https://doi.org/10.1016/j.molmed.2009.07.003

Karczewski, K., Francioli, L., Tiao, G., et al. (2020). The mutational constraint spectrum quantified from variation in 141,456 humans. *Nature*, *581*(7809), 434 - 443. doi: https://doi.org/10.1038/s41586-020-2308-7

Khair, A., & Salvucci, A. (2021). Phenotype expression variability in children with *GABRB3* heterozygous mutations. *Oman Medical Journal*, *36*(2), e240. doi: https://doi.org/10.5001/omj.2021.27

Kothur, K., Holman, K., Farnsworth, E., et al. (2018). Diagnostic yield of targeted massively parallel sequencing in children with epileptic encephalopathy. *Seizure*, *59*, 132 - 140. doi: https://doi.org/10.1016/j.seizure.2018.05.005

Krampfl, K., Maljevic, S., Cossette, P., et al. (2005). Molecular analysis of the a322d mutation in the $GABA_A$ receptor α_1-subunit causing juvenile myoclonic epilepsy. *European Journal of Neuroscience*, *22*(1), 10 - 20. doi: https://doi.org/10.1111/j.1460-9568.2005.04168.x

Lal, D., May, P., Perez-Palma, E., et al. (2020). Gene family information facilitates variant interpretation and identification of disease-associated genes in neurodevelopmental disorders. *Genome Medicine*, *12*(1), 1 - 12. doi: https://doi.org/10.1186/s13073-020-00725-6

Laurie, D., Wisden, W., & Seeburg, P. (1992). The distribution of thirteen $GABA_A$ receptor subunit mRNAs in the rat brain. III. embryonic and postnatal development. *Journal of Neuroscience*, *12*(11), 4151 - 4172. doi: https://doi.org/10.1523/JNEUROSCI.12-11-04151.1992

Leisgen, C., Kuester, M., & Methfessel, C. (2007). The roboocyte. *Methods in molecular biology*, *403*, 87 - 109. doi: https://doi.org/10.1007/978-1-59745-529-9_6

Lerche, H., Shah, M., Beck, H., Noebels, J., Johnston, D., & Vincent, A. (2013). Ion channels in genetic and acquired forms of epilepsy. *The Journal of Physiology*, *591*(4), 753 - 764. doi: https://doi.org/10.1113/jphysiol.2012.240606

Lewis, D., & Gonzalez-Burgos, G. (2006). Pathophysiologically based treatment interventions in schizophrenia. *Nature Medicine*, *12*, 1016 – 1022. doi: https://doi.org/10.1038/nm1478

Liu, X.-B., Coble, J., van Luijtelaar, G., & Jones, E. (2007). Reticular nucleus-specific changes in α_3 subunit protein at GABA synapses in genetically epilepsy-prone rats. *Proceedings of the National Academy of Sciences*, *104*(30), 12512 - 12517. doi: https://doi.org/10.1073/pnas.0705320104

Ma, D., Whitehead, P., Menold, M., et al. (2005). Identification of significant association and gene-gene interaction of GABA receptor subunit genes in autism. *American Journal of Human Genetics*, *77*(3), 377 - 388. doi: https://doi.org/10.1086/433195

Macdonald, R., Kang, J.-Q., & Gallagher, M. (2010). Mutations in $GABA_A$ receptor subunits associated with genetic epilepsies. *The Journal of Physiology*, *588*, 1861 - 1869. doi: https://doi.org/10.1113/jphysiol.2010.186999

Maljevic, S., Keren, B., Aung, Y., et al. (2019). Novel *GABRA2* variants in epileptic encephalopathy and intellectual disability with seizures. *Brain*, *142*(5), e15. doi: https://doi.org/10.1093/brain/awz079

Maljevic, S., Møller, R., Reid, C., et al. (2019). Spectrum of $GABA_A$ receptor variants in epilepsy. *Current Opinion in Neurology*, *32*(2), 183 -190. doi: https://doi.org/10.1097/WCO.0000000000000657

May, P., Girard, S., Harrer, M., et al. (2018). Rare coding variants in genes encoding $GABA_A$ receptors in genetic generalised epilepsies: An exome-based case-control study. *The Lancet Neurology*, *17*(8), 699 - 708. doi: https://doi.org/10.1016/S1474-4422(18)30215-1

McLaren, W., Gil, L., Hunt, S., et al. (2016). The ensembl variant effect predictor. *Genome Biology*, *17*(1), 1 - 14. doi: https://doi.org/10.1186/s13059-016-0974-4

Möhler, H. (2006). $GABA_A$ receptor diversity and pharmacology. *Cell and Tissue Research*, *326*, 505 – 516. doi: https://doi.org/10.1007/s00441-006-0284-3

Møller, R., Wuttke, T., Helbig, I., et al. (2017). Mutations in *GABRB3*: From febrile seizures to epileptic encephalopathies. *Neurology*, *88*(5), 483 - 492. doi: https://doi.org/10.1212/WNL.0000000000003565

National Center for Biotechnology Information. (2021). gamma-aminobutyric acid type a receptor subunit alpha3. *NCBI Database [Internet]*. Retrieved from `https://www.ncbi.nlm.nih.gov/gene?Db=gene&Cmd=DetailsSearch&Term=2556` (accessed: 2021-12-05)

Niturad, C., Lev, D., Kalscheuer, V., et al. (2017). Rare *GABRA3* variants are associated with epileptic seizures, encephalopathy and dysmorphic features. *Brain*, *140*(11),

2879 – 2894. doi: https://doi.org/10.1093/brain/awx236

Nusser, Z., Cull-Candy, S., & Farrant, M. (1997). Differences in synaptic $GABA_A$ receptor number underlie variation in GABA mini amplitude. *Neuron*, *19*(3), 697 - 709. doi: https://doi.org/10.1016/S0896-6273(00)80382-7

Olsen, R., & Sieghart, W. (2016). GABA(A) receptor function and pharmacology in relation to inhibitory neurotransmission. In (pp. Handbook of Experimental Pharmacology, (Vol. 241, pp. 97 - 135)). Springer. doi: https://doi.org/10.1007/164_2016_39

Oyrer, J., Maljevic, S., Scheffer, I., et al. (2018). Ion channels in genetic epilepsy: From genes and mechanisms to disease-targeted therapies. *Pharmacological Reviews*, *70*(1), 142 - 173. doi: https://doi.org/10.1124/pr.117.014456

Papandreou, A., McTague, A., Trump, N., et al. (2016). GABRB3 mutations: a new and emerging cause of early infantile epileptic encephalopathy. *Developmental Medicine Child Neurology*, *58*(4), 416 - 420. doi: https://doi.org/10.1111/dmcn.12976

Pinheiro, P., & Mulle, C. (2008). Presynaptic glutamate receptors: physiological functions and mechanisms of action. *Nature Reviews Neuroscience*, *9*(6), 423 - 436. doi: https://doi.org/10.1038/nrn2379

Pirker, S., Schwarzer, C., Wieselthaler, A., Sieghart, W., & Sperk, G. (2000). $GABA_A$ receptors: Immunocytochemical distribution of 13 subunits in the adult rat brain. *Neuroscience*, *101*(4), 815 - 850. doi: https://doi.org/10.1016/S0306-4522(00)00442-5

Poncer, J., Dürr, R., Gähwiler, B., & Thompson, S. (1996). Modulation of synaptic $GABA_A$ receptor function by benzodiazepines in area CA3 of rat hippocampal slice cultures. *Neuropharmacology*, *35*(9 - 10), 1169 - 1179. doi: https://doi.org/10.1016/S0028-3908(96)00055-X

Rentzsch, P., Witten, D., Cooper, G., Shendure, J., & Kircher, M. (2019). CADD: predicting the deleteriousness of variants throughout the human genome. *Nucleic Acids Research*, *47*(D1), D886 - D894. doi: https://doi.org/10.1093/nar/gky1016

Richards, S., Aziz, N., Bale, S., et al. (2015). Standards and guidelines for the interpretation of sequence variants: a joint consensus recommendation of the american college of medical genetics and genomics and the association for molecular pathology. *Genetics in Medicine*, *17*(5), 405 – 423. doi: https://doi.org/10.1038/gim.2015.30

Rodríguez-Pallares, J., Caruncho, H., López-Real, A., Wójcik, S., Guerra, M., & Labandeira-García, J. (2001). Rat brain cholinergic, dopaminergic, noradrenergic and serotonergic neurons express $GABA_A$ receptors derived from the α_3 subunit.

Receptors Channels, *7*(6), 471 - 478.

Samocha, K., Kosmicki, J., Karczewski, K., et al. (2017). Regional missense constraint improves variant deleteriousness prediction. *BioRxiv*, *148353*. doi: https://doi.org/10.1101/148353

Scheffer, I., Berkovic, S., Capovilla, G., et al. (2017). ILAE classification of the epilepsies: Position paper of the ILAE commission for classification and terminology. *Epilepsia*, *58*, 512 - 521. doi: https://doi.org/10.1111/epi.13709

Sieghart, W., & Sperk, G. (2002). Subunit composition, distribution and function of $GABA_A$ receptor subtypes. *Current Topics in Medicinal Chemistry*, *2*(8). doi: https://doi.org/10.2174/1568026023393507

Srivastava, S., Cohen, J., Pevsner, J., et al. (2014). A novel variant in GABRB2 associated with intellectual disability and epilepsy. *American journal of medical genetics Part A*, *164*(11), 2914-2921. doi: https://doi.org/10.1002/ajmg.a.36714

Steudle, F., Rehman, S., Bampali, K., et al. (2020). A novel de novo variant of *GABRA1* causes increased sensitivity for GABA in vitro. *Scientific Reports*, *10*, 2379. doi: https://doi.org/10.1038/s41598-020-59323-6

Syed, P., Durisic, N., Harvey, R., Sah, P., & Lynch, J. (2020). Effects of $GABA_A$ receptor α_3 subunit epilepsy mutations on inhibitory synaptic signaling. *Frontiers in Molecular Neuroscience*, *13*, 227. doi: https://doi.org/10.3389/fnmol.2020.602559

Taliun, D., Harris, D., Kessler, M., et al. (2021). Sequencing of 53,831 diverse genomes from the NHLBI TOPMed program. *Nature*, *590*(7845), 290 - 299. doi: https://doi.org/10.1038/s41586-021-03205-y

Tasker, J., & Dudek, F. (1991). Electrophysiology of GABA-mediated synaptic transmission and possible roles in epilepsy. *Neurochemical Research*, *16*, 251 – 262. doi: https://doi.org/10.1007/BF00966088

Terzic, B., Davatolhagh, M., Ho, Y., et al. (2021). Temporal manipulation of cdkl5 reveals essential postdevelopmental functions and reversible cdkl5 deficiency disorder–related deficits. *The Journal of Clinical Investigation*, *131*(20). doi: https://doi.org/10.1172/JCI143655.

Thompson, A., Lester, H., & Lummis, S. (2010). The structural basis of function in cys-loop receptors. *Quarterly Reviews of Biophysics*, *43*(4), 449 - 499. doi: https://doi.org/10.1017/S0033583510000168

Traynelis, J., Silk, M., Wang, Q., et al. (2017). Optimizing genomic medicine in epilepsy through a gene-customized approach to missense variant interpretation. *Genome Research*, *27*(10), 1715 - 1729. doi: https://doi.org/10.1101/gr.226589.117

UniProt Consortium. (2021). *Gamma-aminobutyric acid receptor subunit alpha-3.* Re-

trieved 2021-11-27, from https://www.uniprot.org/uniprot/P34903

Unwin, N. (1993). Neurotransmitter action: Opening of ligand-gated ion channels. *Cell*, *72*, 31 - 41. doi: https://doi.org/10.1016/S0092-8674(05)80026-1

Wallace, R., Marini, C., Petrou, S., et al. (2001). Mutant $GABA_A$ receptor γ_2-subunit in childhood absence epilepsy and febrile seizures. *Nature Genetics*, *28*, 49 - 52. doi: https://doi.org/10.1038/ng0501-49

Weber, Y., & Lerche, H. (2008). Genetic mechanisms in idiopathic epilepsies. *Developmental Medicine & Child Neurology*, *50*, 648 - 654. doi: https://doi.org/10.1111/j.1469-8749.2008.03058.x

Wiedenmann, B., Franke, W., Kuhn, C., Moll, R., & Gould, V. (1986). Synaptophysin: a marker protein for neuroendocrine cells and neoplasms. *Proc Natl Acad Sci U S A*, *83*(10), 3500 - 3504. doi: https://doi.org/10.1073/pnas.83.10.3500

World Health Organization. (2021). *Epilepsy*. Retrieved 2021-11-27, from https://www.who.int/health-topics/epilepsy#tab=tab_1

Yuan, H., Low, C., Moody, O., Jenkins, A., & Traynelis, S. (2015). Ionotropic GABA and glutamate receptor mutations and human neurologic diseases. *Molecular Pharmacology*, *88*, 203 – 217. doi: https://doi.org/10.1124/mol.115.097998

9 Statement of Authorship

I, the Author, confirm that the work presented here has been performed and written solely by myself except where explicitly identified as the contrary. External thoughts and ideas as well as sources and other aids are made recognizable as such without exception.

10 Selbstständigkeitserklärung

Die Arbeit wurde im Hertie-Institut für klinische Hirnforschung unter Betreuung von Prof. Dr. med. Holger Lerche, Dr. Ulrike Hedrich-Klimosch und Mahmoud Koko Musa durchgeführt. Die Konzeption der Studie erfolgte in Zusammenarbeit mit Prof. Dr. med. Holger Lerche und Dr. Ulrike Hedrich-Klimosch. Die statistische Auswertung erfolgte nach Beratung mit Dr. Ulrike Hedrich-Klimosch und Mahmoud Koko Musa durch mich. Ich versichere, das Manuskript selbständig verfasst zu haben und keine weiteren als die von mir angegebenen Quellen verwendet zu haben. Die aus fremden Quellen direkt oder indirekt übernommenen Gedanken sind ausnahmslos als solche kenntlich gemacht.

Tübingen, July 15, 2024